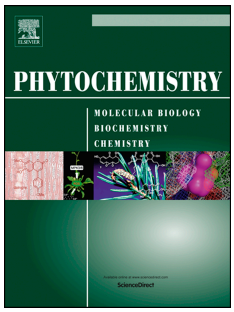


# Auxin and light-mediated regulation of growth, morphogenesis, and alkaloid biosynthesis in *Crinum* x *powellii* 'Album' callus

Manoj Koirala, Karen Cristine Goncalves dos Santos, Sarah-Eve Gélinas, Simon Ricard, Vahid Karimzadegan, Basanta Lamichhane, Nuwan Sameera Liyanage, Natacha Merindol, Isabel Desgagné-Penix

PII: S0031-9422(23)00299-6

DOI: https://doi.org/10.1016/j.phytochem.2023.113883

Reference: PHYTO 113883

To appear in: *Phytochemistry*

Received Date: 24 July 2023

Revised Date: 27 September 2023

Accepted Date: 29 September 2023

Please cite this article as: Koirala, M., Cristine Goncalves dos Santos, K., Gélinas, S.-E., Ricard, S., Karimzadegan, V., Lamichhane, B., Sameera Liyanage, N., Merindol, N., Desgagné-Penix, I., Auxin and light-mediated regulation of growth, morphogenesis, and alkaloid biosynthesis in *Crinum* x *powellii* 'Album' callus, *Phytochemistry* (2023), doi: https://doi.org/10.1016/j.phytochem.2023.113883.

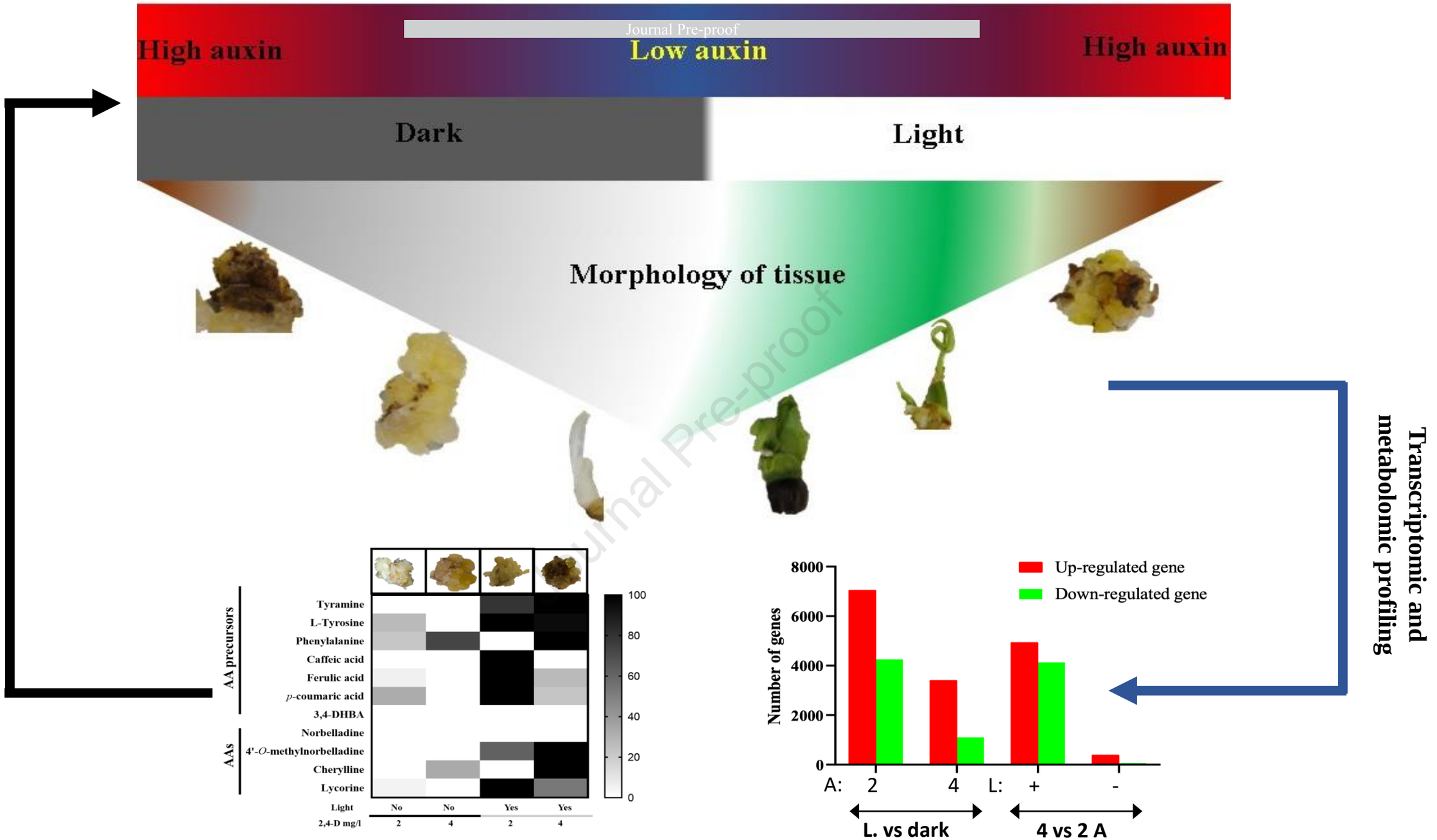


Targeted metabolomic and transcriptomic studies reveal the effect of auxin and light on the growth, morphogenesis, and alkaloid biosynthesis in *C.* x *powellii* "Album". An investigation of the effects of different growth factors on *in vitro* tissues helps to better understand the balance between stress and growth, and eventually, further fine-tune alkaloid production (L: light, A: auxin 2,4-D in mg/L).

# Auxin and light-mediated regulation of growth, morphogenesis, and alkaloid biosynthesis in *Crinum* x *powellii* 'Album' callus

Manoj Koirala [1], Karen Cristine Goncalves dos Santos [1], Sarah-Eve Gélinas [1], Simon Ricard [1], Vahid Karimzadegan [1], Basanta Lamichhane [1], Nuwan Sameera Liyanage [1], Natacha Merindol [1], Isabel Desgagné-Penix [1,2*]

[1] Department of Chemistry, Biochemistry and Physics, Université du Québec à Trois-Rivières, Trois-Rivières, QC, Canada

[2] Plant Biology Research Group, Trois-Rivières, Québec, Canada

* Corresponding author's email address: Isabel.Desgagne-Penix@uqtr.ca

## Abstract

*Crinum* x *powellii* 'Album' belongs to the Amaryllidaceae medicinal plant family that produces a range of structurally diverse alkaloids with potential therapeutic properties. The optimal conditions for *in vitro* tissue growth, morphogenesis, and alkaloid biosynthesis remain unclear. Auxin and light play critical roles in regulating plant growth, development, and alkaloid biosynthesis in several Amaryllidaceae plants. Here, we have succeeded in showing, for the first time, that the combination of auxin and light significantly influence *C.* x *powellii* "Album" *in vitro* tissue growth, survival, and morphogenesis compared to individual treatments. Furthermore, this combination also upregulates the expression of alkaloid biosynthetic genes and led to an increase in the content of certain alkaloids, suggesting a positive impact on the defense and therapeutic potential of the calli. Our findings provide insights into the regulation of genes involved in alkaloid biosynthesis in *C.* x *powellii* "Album" callus and underline the potential of auxin and light as tools for enhancing their production in plants. This study provides a foundation for further exploration of *C.* x *powellii* "Album" calli as a sustainable source of bioactive alkaloids for pharmaceutical and agricultural applications. Furthermore, this study paves the way to the discovery of the biosynthetic pathway of specialized metabolites from *C.* x *powellii* "Album", such as cherylline and lycorine.

**Keywords**: Amaryllidaceae Alkaloids, stress, transcriptomic study, AAs biosynthesis pathway

## 1. Introduction

Plant natural products have been an abundant source of chemical compounds for drug discovery (Rates, 2001). Such molecules, whose biosynthesis is essential for plants to adapt and to interact with harsh ecological environments, are defined as plant specialized metabolites (SMs) (Jacobowitz and Weng, 2020). Plant-derived alkaloids comprise one of the largest classes of SMs, reported in almost 20% of plants. Among them, alkaloids that are exclusively reported in the Amaryllidaceae plant family are known as Amaryllidaceae alkaloids (AAs) (Desgagné-Penix, 2020; Dewick, 2009; Jin and Yao, 2019; Lewis, 1996; Martin, 1988; Singh and Desgagne-Penix, 2015). AAs have chemotherapeutical effects on humans. For instance, galanthamine is marketed for the treatment of Alzheimer's disease, lycorine has cytotoxic and antiviral properties (Ieven et al., 1982; Nair and van Staden, 2023; Tallini et al., 2017), and cherylline is a non-cytotoxic antiviral compound (Ka et al., 2020; Ka et al., 2021b). The *Crinum* genus from the Amaryllidaceae family, contains more than 130 species widely distributed among subtropical and tropical regions. Plants from this genus are used in traditional medicine as they display antitumor, immunostimulant, analgesic, antiviral, and antibacterial properties (Fennell and van Staden, 2001). Accordingly, several *Crinum* species produce both cherylline and lycorine, together with copious AAs structures displaying a wide range of pharmacological activities (Abd el Hafiz et al., 1991; Fennell et al., 2003; Ka et al., 2021b; Refaat et al., 2012; Tallini et al., 2018). *C.* x *powellii* "Album" (swamp lily) is an interspecies hybrid plant of *C. moorei* and *C. bulbispermum*, from which a number of AAs have been reported, including cherylline, lycorine, 1-*O*-acetyl-lycorine, cripowellin, and ismine, emphasizing its potential pharmacological interest (Brossi et al., 2002; Nino et al., 2007; Velten et al., 1998).

In Amaryllidaceae, most of the metabolic enzymatic reactions yielding different AAs are not known. The biosynthesis involves the shikimate pathway that produces precursor aromatic amino acids, including L-phenylalanine and L-tyrosine (Fig. 1). On one hand, L-phenylalanine follows the phenylpropanoid pathway to generate 3,4-dihydoxybenzylaldehyde (Desgagné-Penix, 2020; Koirala et al., 2022). On the other hand, tyrosine is decarboxylated into tyramine under the action of tyrosine decarboxylase (TYDC) enzymes (Hu et al., 2021). Reuniting both precursors, norbelladine synthase (NBS) (Singh et al., 2018; Tousignant et al., 2022) and norcraugsodine reductase (Kilgore et al., 2016) catalyze the condensation and reduction of tyramine and 3,4-dihydroxybenzyladehyde into norcraugsodine and then norbelladine (Majhi et al., 2022), the latter

being the key intermediate compound of the pathway. Biochemical modifications of norbelladine or of its precursors by *O*-methyltransferase (*O*MT), and further modification by phenol-coupling reactions by cytochrome P450 (CYP), generate a diverse type of AAs. Up to date, more than 650 AAs of different ring types and biogenic origin such as norbelladine-, cherylline-, galanthamine-, crinine-, lycorine-types have been reported (Tallini et al., 2017).

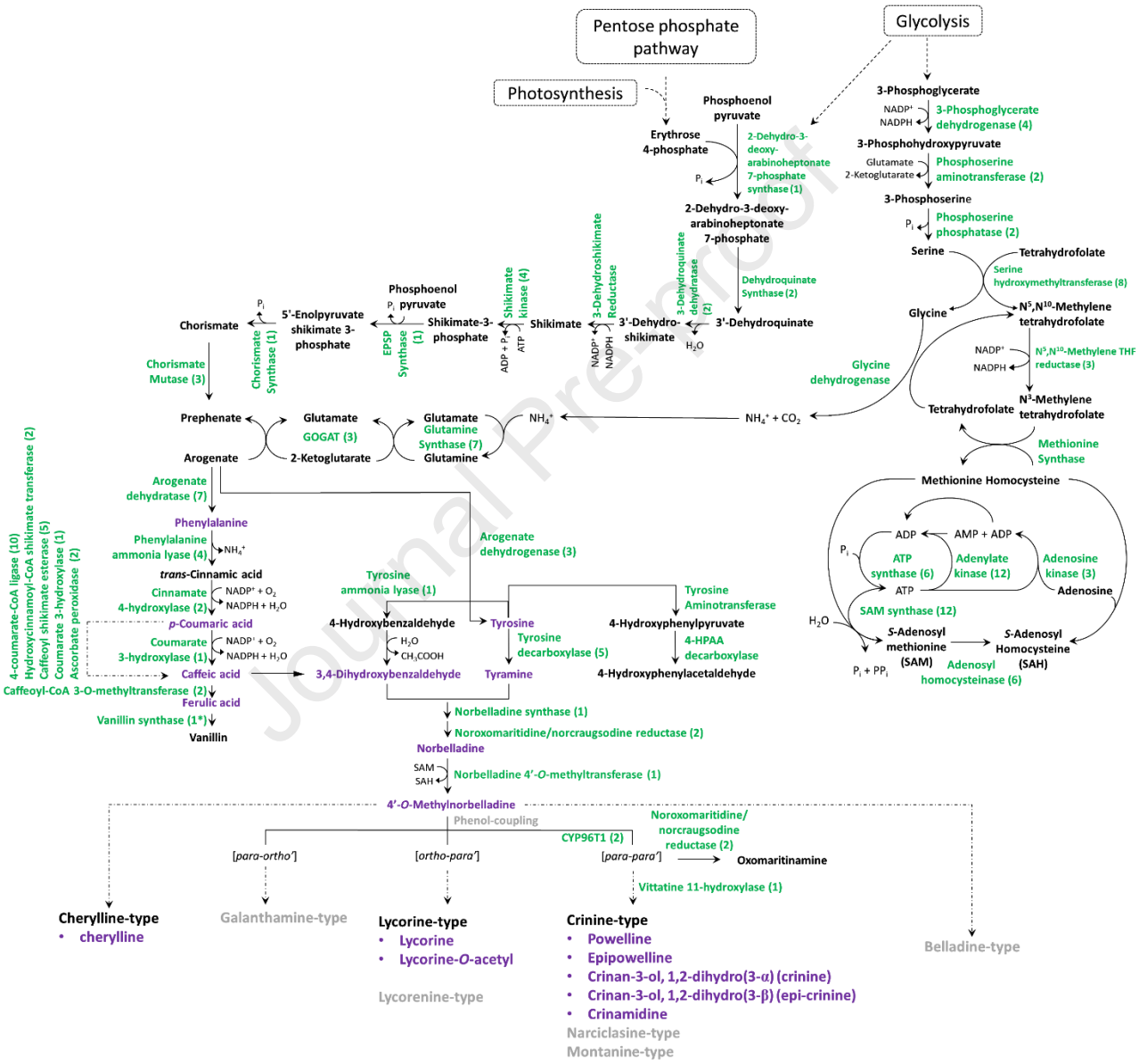


**Fig. 1** Proposed metabolic pathway leading to Amaryllidaceae alkaloids. Black arrow represents one reaction whereas dotted arrow represents several reactions. Enzyme catalyzing key reactions identified in *C* x *powelli* "Album" transcriptome in this study are written in green. Metabolites written in purple were detected in this study in *C* x *powelii* "Album" extracted tissues whereas Amaryllidaceae alkaloid types written in gray were not detected. Numbers in small bracket represent the number of complete transcripts identified in the transcriptome of *C*. x *powellii* "Album".

Unfortunately, AA biosynthesis and accumulation occur at low levels *in planta*, varying with developmental stages, tissues and seasonal changes (Hotchandani et al., 2019; Lubbe et al., 2013). This issue impairs the commercial application of AAs, because their production requires large volumes of plant material (Brossi et al., 2002; Koirala et al., 2022; Lubbe et al., 2013). A successful alternative strategy includes the use of *in vitro* culture of specific plant tissues to produce SMs have been described before. The initiation and establishment of such methodology are influenced by several factors, such as exogenous supply of phytohormones and culture conditions (Gaba, 2005; Trujillo Chacón et al., 2023). Auxins are phytohormones known to induce cell elongation and to regulate diverse processes in plants, such as trophic responses to light and gravity, general shoot and root architecture, organogenesis, and growth in tissue culture. Exogenous supplies of auxins can greatly impact tissue differentiation and AA accumulation (Ptak et al., 2013). The exposure to light is also an important parameter for plant *in vitro* culture. Recently, the effects of photoperiod on *in vitro* cultures of *Narcissus tazetta* showed that both tissue differentiation and alkaloid accumulation varied in relation to light conditions (Rahimi Khonakdari et al., 2020). Lastly, in addition to its use as a mean of production of SMs, *in vitro* plant tissue culture technology can provide a powerful platform to uncover biosynthetic pathways and to generate a homogeneous sample that can be used in further studies (Gallego et al., 2018).

In this study, we developed the *in vitro* culture of *C.* x *powellii* "Album" varying both light and auxins concentrations. Then, to explore the effect of different factors on the biosynthesis of AAs, we performed a comparative transcriptomic study between alkaloid-producing and non-producing callus generated with four culture conditions, varying both auxin treatment and light exposure. This study presents the first transcriptome analysis of a species that produce cherylline (Fig 1).

## 2. Results

### 2.1 *Crinum* x *powellii* "Album" clusters with *Crinum* species endemic to South Africa

To genotype *C.* x *powellii* "Album" (Fig. 2a), a partial *ITS2* region was amplified from genomic DNA (Ka et al., 2021a; Wang and Chen, 2007). The phylogenetic analysis was performed with 10 different species of the *Crinum* genus, using *Amaryllis belladonna* as outgroup (Fig. 2b). Close analysis of the *ITS2* region reveals two subclades, (i) from *C. stuhlmannii* to *C. forbesii* highlighted in yellow color and (ii) from *C. yemenense* to *C. oliganthum* highlighted in blue color, which is consistent with Meerow et al. (2003). Subclade (i) includes mostly African species together with *C. flaccidum*, endemic of Australia. *C.* x *powellii* clusters inside this group, more specifically with the South African endemics *C. stuhlmannii*, and *C. bulbispermum*, and *C. moorei* from which it derives. Subclade (ii) is formed by the American clade, together with tropical and North African species.

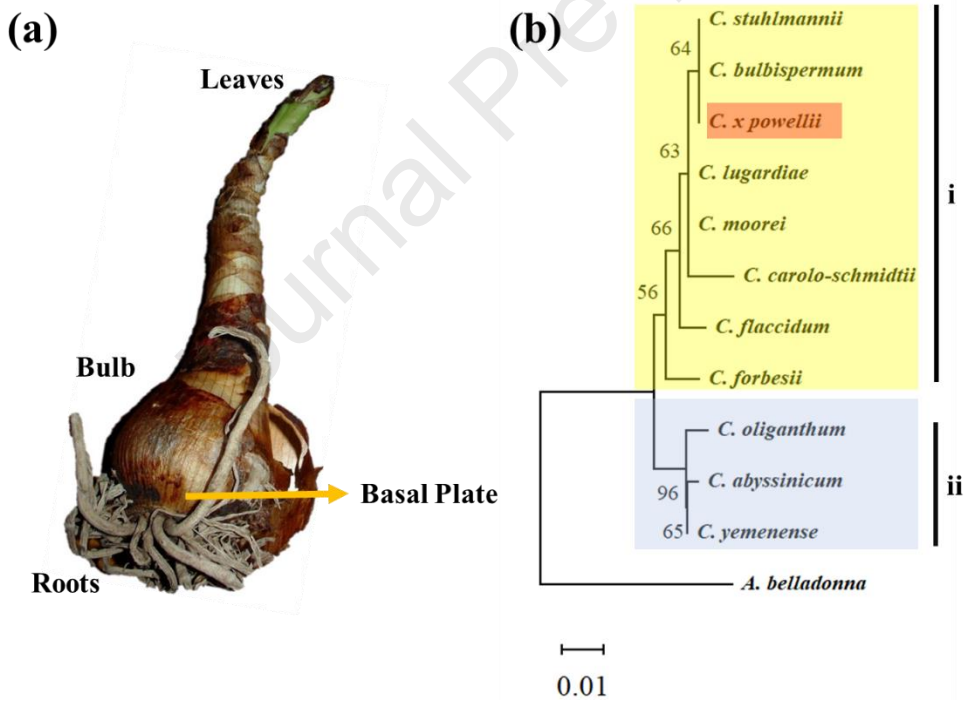


**Fig. 2** (a) *C.* x *powellii* "album" tissues used in this study. (b) Genotyping of *C.* x *powellii* "Album". The phylogenetic analysis was performed using Molecular Evolutionary genetic analysis (MEGA 11.0.3) software. The evolutionary history was inferred using the Neighbor-Joining method and the optimal tree is shown. The percentage of replicate trees in which the associated taxa clustered together in the bootstrap test (1000 replicates) are shown next to the branches. The tree is drawn to scale, with branch

lengths in the same units as those of the evolutionary distances used to infer the phylogenetic tree. The evolutionary distances were computed using the p-distance method and are in the units of the number of base differences per site. This analysis involved *ITS2* region from *C*. x *powellii* "Album", ten ITS2 region nucleotide sequences from different *Crinum* species including (*C. abyssinicum* (AY139117.1), *C. oliganthum* (AY139142.1), *C. lugardiae* (JX464264.1), *C. yemenense* (AY139151.1), *C. moorei* (AY139141.1), *C. stuhlmannii* (JX464267.1), *C. carolo-schmidtii* (AY139125.1), *C. forbesii* (AY139133.1), *C. flaccidum* (AY139132.1), *C. bulbispermum* (AY139123.1) ) and *A. belladonna* (JX464257.1) as a out-group. *C*. x *powellii* "Album" is highlighted in red. Close analysis of the *ITS2* region reveals two subclades; (i) from *C. stuhlmannii* to *C. forbesii* highlighted in yellow and (ii) from *C. yemenense* to *C. oliganthum* highlighted in blue.

### 2.2 *Crinum* x *powellii* "Album" *in vivo* tissues are enriched in crinine-, lycorine- and cherylline-type alkaloids.

Next, we explored the metabolite profile of crude methanolic extracts of *C.* x *powellii* "Album" tissues, including roots, basal plates, bulbs, and young leaves (Fig. 2a). The GC-MS analysis showed the presence of 52 peaks, and the identity of some AAs was confirmed by comparing fragmentation pattern of detected compound with the NIST library 0.5 (Table S1). Overall, three different types of AAs were detected in *C.* x *powellii* "Album", namely crinine-type (powelline, epipowelline, crinine acetate and crinine), lycorine-type (lycorine and lycorine-*O*-acetate) and cherylline-type (cherylline) (Table 1; Fig. 3; and Fig. S2). Lycorine was detected in all analyzed organs of *C.* x *powellii* "Album", however, its *O*-acetylated derivative was detected only in leaves. Crinine-type alkaloids were detected in different parts of the plant. Cherylline was detected in all studied organs, except in the leaves. Basal plates and leaves contained the most diversified profile of alkaloids (Table 1).

**Table 1** Amaryllidaceae alkaloid detection in different *C.* x *powellii* "Album" samples using GC-MS analysis. The number of m/z observed corresponds to the number of peaks detected in the samples. n.a: not applicable. Shown are only tissues and conditions in which alkaloids were specifically detected. Experiments were done in triplicates. *, ** and *** indicate the number of replicates (i.e., one, two or three out of three) where the corresponding metabolites were detected and identified. Our detection threshold consisted of a NIST05 hit > 90 % at a given retention time (see Table S1). Numbers in small brackets refer to Table S1 alkaloids and Fig. S2 peaks.

| **Type** | **Light** | **Type of auxin (concentration)** | **Type of tissue** | **Number of m/z observed** | **Lycorine** | | **Crinine** | | | | | | **Cherylline** |
|---|---|---|---|---|---|---|---|---|---|---|---|---|---|
| | | | | | Lycorine (**8**) | Lycorine -*O*-acetate (**7**) | Epipowelline (**6**) | Crinan-3-ol,1,2-didehydro(3-alpha) (**1**) | Crinamidine (**9**) | Crinine acetate (**4**) | Crinan-3-ol,1,2-didehydro(3-beta) (**2**) | Powelline (**5**) | Cherylline (**3**) |
| *In vivo* | n.a. | n.a. | Leave | 32 | ** | * | * | * | | *** | ** | | |
| | | | Bulb | 23 | *** | | | *** | | | | *** | *** |
| | | | Root | 22 | *** | | | *** | | | | *** | *** |
| | | | Basal plate | | *** | | | *** | | *** | | *** | *** |
| *In vitro* | - | NAA(2 mg/L) | Indirect bulblet | 13 | | | | | | | | ** | |
| | + | NAA (2 mg/L) | Callus | 15 | | | | * | | | | *** | |
| | | | Indirect shoot | 19 | ** | | | * | *** | | | *** | *** |
| | | NAA (4 mg/L) | Callus | 15 | | | | | | | | ** | |
| | | | Indirect shoot | 15 | ** | * | | | ** | | | ** | ** |
| | | NAA (8 mg/L) | Callus | 13 | | | | | | | | * | |
| | | | Indirect shoot | 19 | ** | | * | ** | *** | | | *** | *** |

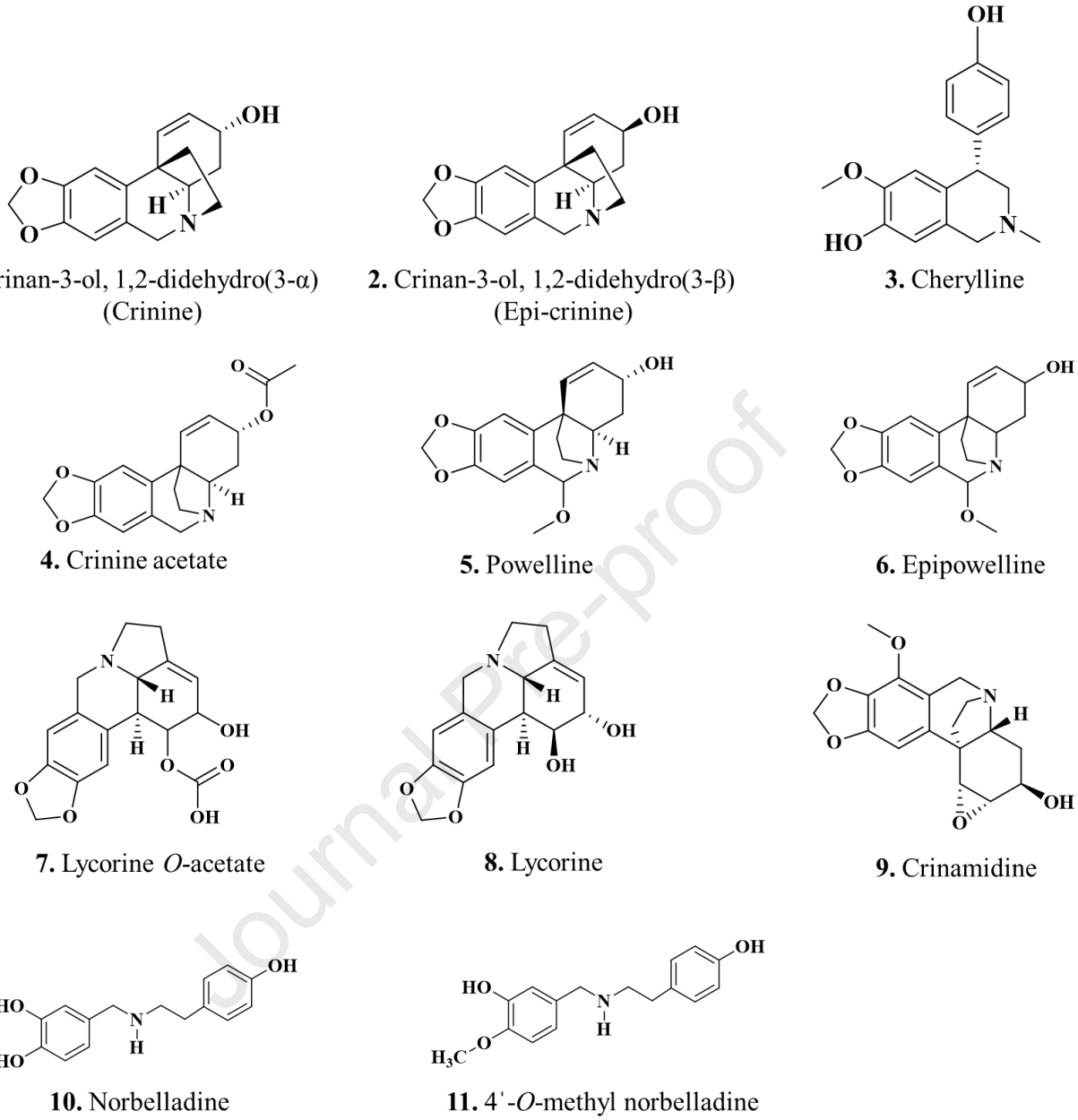


139

140 **Fig. 3** Structure of alkaloids from *C.* x *powellii* "Album". Alkaloids 1 to 9 were detected using GC-MS analysis,
141 compound 1, 3 and 8 were detected in both GC-MS and LC-MS/MS analyses whereas compound 10 and 11 were only
142 detected using LC-MS/MS analysis of *C.* x *powellii* "Album" sample . Relative quantity of compound 1, 8, 10 and
143 12 were determined using LC-MS/MS.

144 **2.3 Light and auxin greatly affect *in vitro* tissue survival and morphogenesis.**

145 To develop *in vitro* culture of *C.* x *powellii* "Album", twin scale explants were extricated from
146 bulbs after surface sterilization. Explants grown in light and dark conditions displayed distinct
147 morphologies. When grown in dark, explants were mostly white. By contrast, upon exposure to

light, they were mainly green and brownish, depending on the type of auxin used. We observed a 5.60-fold increase in browning of explant during *in vitro* culture in light compared to dark condition (Fig. S3). Browning of most of explant was followed by death of explant or callus**.**

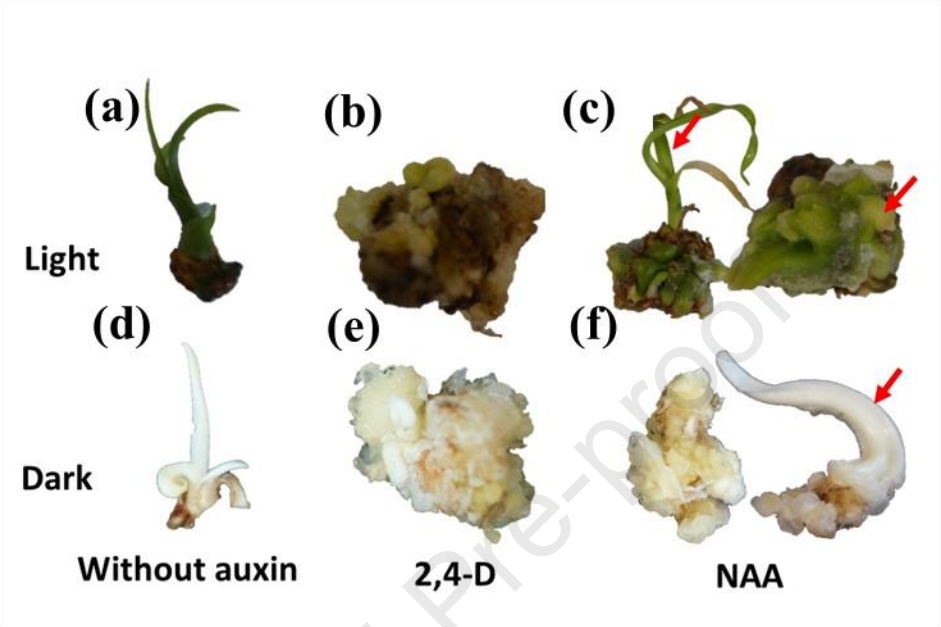


**Fig. 4** Different types of tissue generated from the *in vitro* culture of *C.* x *powellii* "Album". (a), (b) & (c) represent tissues developed in light conditions; (d), (e) & (f) represent tissues generated in the dark condition. (a) & (d), tissues generated without auxin (direct organogenesis); (b) & (e), tissues generated with 2,4-D (callus formation); (c) & (f), tissues generated with NAA (red arrow indicates indirect organogenesis). Shown are representative pictures of 6 months old tissues for each mentioned condition. Pictures were taken under the laminar hood from callus and explants grown in Petri dishes, they displayed approximately the same size.

Following this initial phase of culture, different types of tissues continued to develop depending on the conditions and types of hormones, over the 6 months study period of *C.* x *powellii* culture (Fig. 4; Table S3). In absence of auxin, no callus induction was observed, but direct organogenesis (direct shoot formation) occurred for 100% of explants. Although overall survival rate of explants grown in light was lower (Fig. S3), tissues generated in darkness without auxin only survived for short periods, starting to die after 20-22 weeks of culture. Induction of callus was observed after 3-4 weeks, occurring more rapidly with media supplemented with 2,4-D (at every concentration), regardless of light exposure. When media were supplemented with NAA, callus induction occurred in 4-6 weeks, depending on its concentration. The type of auxin also affected the type of tissues generated. Initial callus morphogenesis in presence of 2,4-D was globular, while NAA led to a swelling-type of callus. In the case of 2,4-D, explants grew as undifferentiated tissues (callus,

100% of explants) regardless of its concentration and light exposure, whereas light played a role in the explant development when NAA was supplied as auxin. In the light-exposed condition, with 2 and 4 mg/L of NAA, shoot generation occurred within 8 weeks, whereas with 8 mg/L, it took 14 weeks for tissue to become differentiated. In dark condition, tissue differentiation was observed on the $10^{th}$ week of culture when supplied with 2 and 4 mg/L of NAA; however, no shoot formation was seen with higher concentration of this hormone.

### 2.4 Light increases the production of metabolites in *in vitro* tissue

To understand the alkaloid producing capability of *in vitro* tissues, GC-MS analysis of methanolic extracts was performed. Noteworthy, fewer AAs were identified from undifferentiated tissues compared to *in vivo* or *in vitro* differentiated samples (Table 1). Another remarkable difference was the near absence of AA detection in tissues grown in the dark (with or without 2,4-D), compared to *in vivo* and light-exposed tissues, and NAA-treated, respectively. Four to fourteen metabolite peaks were detected in samples grown in dark condition, depending on auxin concentration. However, powelline was the only alkaloid identified in differentiated tissue (induced bulblet) generated in the culture supplemented with 2 mg/L of NAA in the dark (Table 1). By contrast, 8 to 19 metabolite peaks were observed in *in vitro* tissue samples exposed to light. Tissue differentiation following NAA treatment was associated with an increase in AA detection in cultures exposed to light. In contrast to tissue growth in dark conditions, powelline was detected in all calli grown exposed to light with any of the tested NAA concentrations (Table 1). Interestingly, the types of AAs detected in *in vitro* tissues generated from the light with NAA were similar to the AAs detected from *in vivo* tissue. All three types of AAs, *i.e.*, lycorine-, crinine- and cherylline-type, were identified from differentiated tissues treated with NAA and exposed to light.

### 2.5 Lycorine and cherylline are triggered by light and 2,4-D in undifferentiated tissues

AAs were undetectable (below lower limits of quantitation) in several *in vitro* tissues following GC-MS analysis, especially those treated with 2,4-D. To get a broader and more sensitive view of *in vitro* tissues AA profile, we performed targeted metabolite analysis using LC-MS/MS. In general, a similar profile of metabolite enrichment according to tissue differentiation (compounds are more abundant in shoots), light exposure and auxin (NAA) treatment was observed using both methods (Fig. S4). However, LC-MS/MS allowed for the sensitive detection of alkaloids in callus grown in darkness. Metabolites such as five AAs (*i.e.* norbelladine, 4'-*O*-methylnorbelladine,

cherylline, lycorine and crinine) and six precursors (*i.e.*, caffeic acid, ferulic acid, L-tyrosine, *p*-coumaric acid, phenylalanine, and tyramine) were identified based on their retention time and fragmentation pattern compared to available authentic standards (Fig. 3, Fig. 5; Fig. S4). In callus, the accumulation of these metabolites of interest was mostly affected by light, and then by 2,4-D (Fig. 5). Hence, we focused our analysis on the combination of these two conditions. 4'-*O*-methylnorbelladine was detected in tissues exposed to light regardless of concentration of 2,4-D, however its accumulation was 3-fold higher in tissues grown with 4 compared to 2 mg/L of 2,4-D. The accumulation of lycorine was almost 2-fold higher in tissue cultured with 2 compared to 4 mg/L of 2,4-D. Cherylline was not detected in callus obtained from tissues cultured with 2 mg/L of 2,4-D, but was detected at 4 mg/L of 2,4-D, with an accumulation 2.5-fold higher in light compared to dark condition (Fig. 5; Fig. S4).

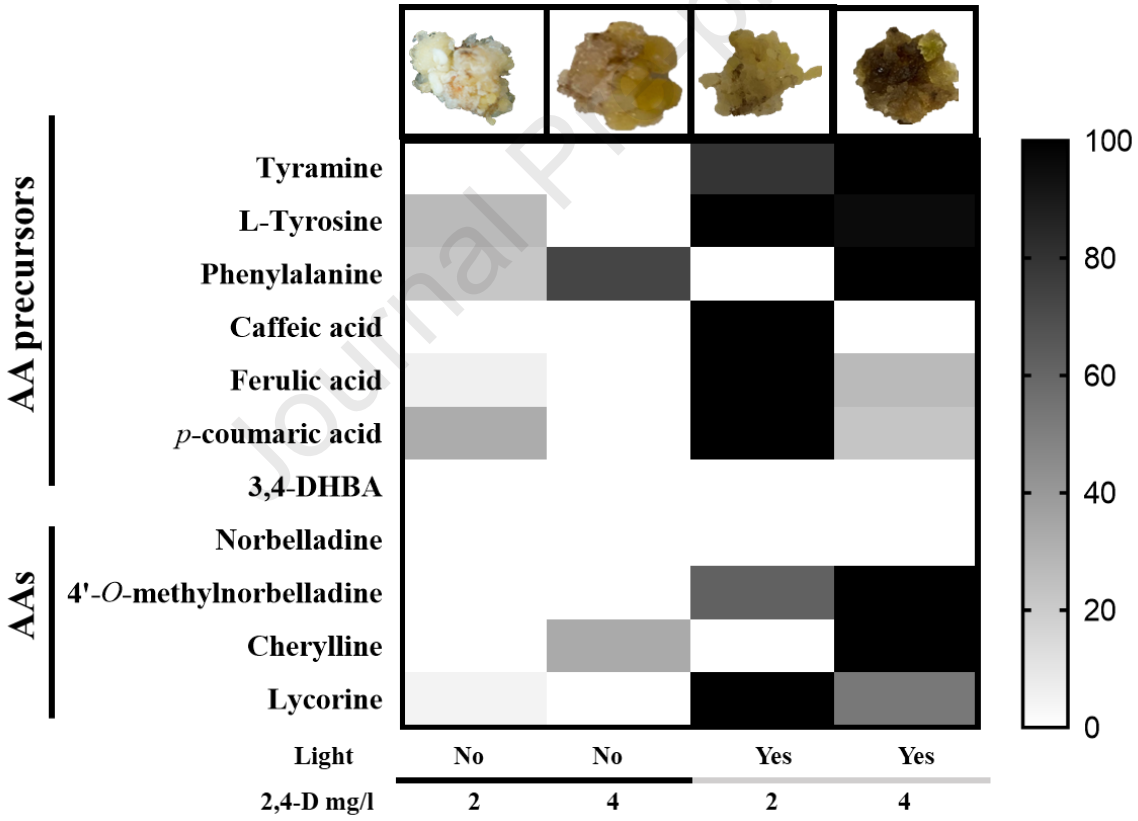


**Fig. 5** LC-MS/MS analysis of targeted metabolites in tissue generated from *in vitro* culture of *C.* x *powellii* "Album". On top, callus developed during *in-vitro* culture conditions, from left to right: dark:2 mg/L of 2,4-D, dark:4 mg/L of 2,4-D, light:2 mg/L of 2,4-D and light:4 mg/L of 2,4-D. Heatmap shows the relative abundance of target metabolites in tissue culture of *C.* x *powellii* "Album". Relative abundance corresponds to the mean value of three independent replicated values normalized to the sample with the highest level for each compound. The condition in which the

highest quantity of a specific compound was detected is shown as the most intense box. Pictures were taken under the laminar hood from callus grown in Petri dishes, they displayed approximately the same size.

### 2.6 *De novo* transcriptomic assembly of *C* x *powellii* "Album"

To get insight into the biosynthesis route and uncover the genes involved in lycorine and cherylline production in *C.* x *powellii* "Album", we performed RNA sequencing (RNA-seq) from selected callus of *C.* x *powellii* "Album" cultured in light and dark conditions, with 2 mg/L or 4 mg/L of 2,4-D. The 8 mg/L of 2,4-D treatment was not included as it did not yield enough tissue for further analysis. Also, the NAA treatment was excluded since the organogenesis occurred in light condition only, which would result in an additional variable dimension. Furthermore, to generate a complete view of the species transcriptome, we also included the RNA-seq data obtained from *in vivo* tissues. Altogether, a total of 1 240 830 608 raw reads were generated (Table S4). These were cleaned up using optimized fastp software, according to initial quality assessment performed with FastQC, resulting in 1 162 489 247 clean reads. These were assembled using Trinity software, yielding 1 261 988 of trinity transcripts and 785 475 trinity genes. BUSCO analysis revealed that 90.7% of the orthologs in the embryophyte database were found complete in the transcriptome of *C.* x *powellii* "Album". The assembly had N50 of 1 033, with mean and median contig lengths of 364 and 658.04 respectively (Table S4). In total, 133 843 transcripts were annotated using Pfam and Uniprot databases.

Next, the gene-size distribution, GO and COG analysis of assembled *C.* x *powellii* "Album" transcriptome were generated and the GO term annotation of the transcripts based on UniProt, SwissProt and Pfam annotations was obtained (Fig. S5). Most genes were associated with "binding" (GO:0005488, molecular function). The second largest number of transcripts were annotated with GO terms belonging to "cellular process" (GO:0009987, biological process) (Fig. S5). There were fewer transcripts annotated with cellular component GO terms. Based on the sequence homology, 1008 assemble genes had COG (Clusters of Orthologous Genes) functional classification, resulting into 24 categories (Fig. S5). "Energy production and conversion" was the most common category followed by "general function", whereas "cytoskeleton", "extracellular structure", "RNA processing and modification" and "chromatin structure and dynamic" were the ones with fewer transcripts.

## 2.7 A combination of light and 2,4-D modulates the expression of photosynthesis- and stress response-related gene categories.

To elucidate the effect of different factors in the underlying regulatory processes, we performed a comparative transcriptomic study between AAs producing and non-producing callus cultures in light and dark conditions, with 2 and 4 mg/L of 2,4-D. Principal component analysis of transcriptomic data revealed three main clusters well separated from one another (Fig. S6). The exposure to light played a dominant role in the gene expression profile of the samples than the concentration of 2,4-D, and calli grown in the dark were more homogenous than when exposed to light. Two sub-clusters were observed in the dark-grown group according to the concentration of auxin used. Strikingly, in light-exposed callus, the concentration of the phytohormone played a greater role in the gene expression profiles, generating two distant clusters.

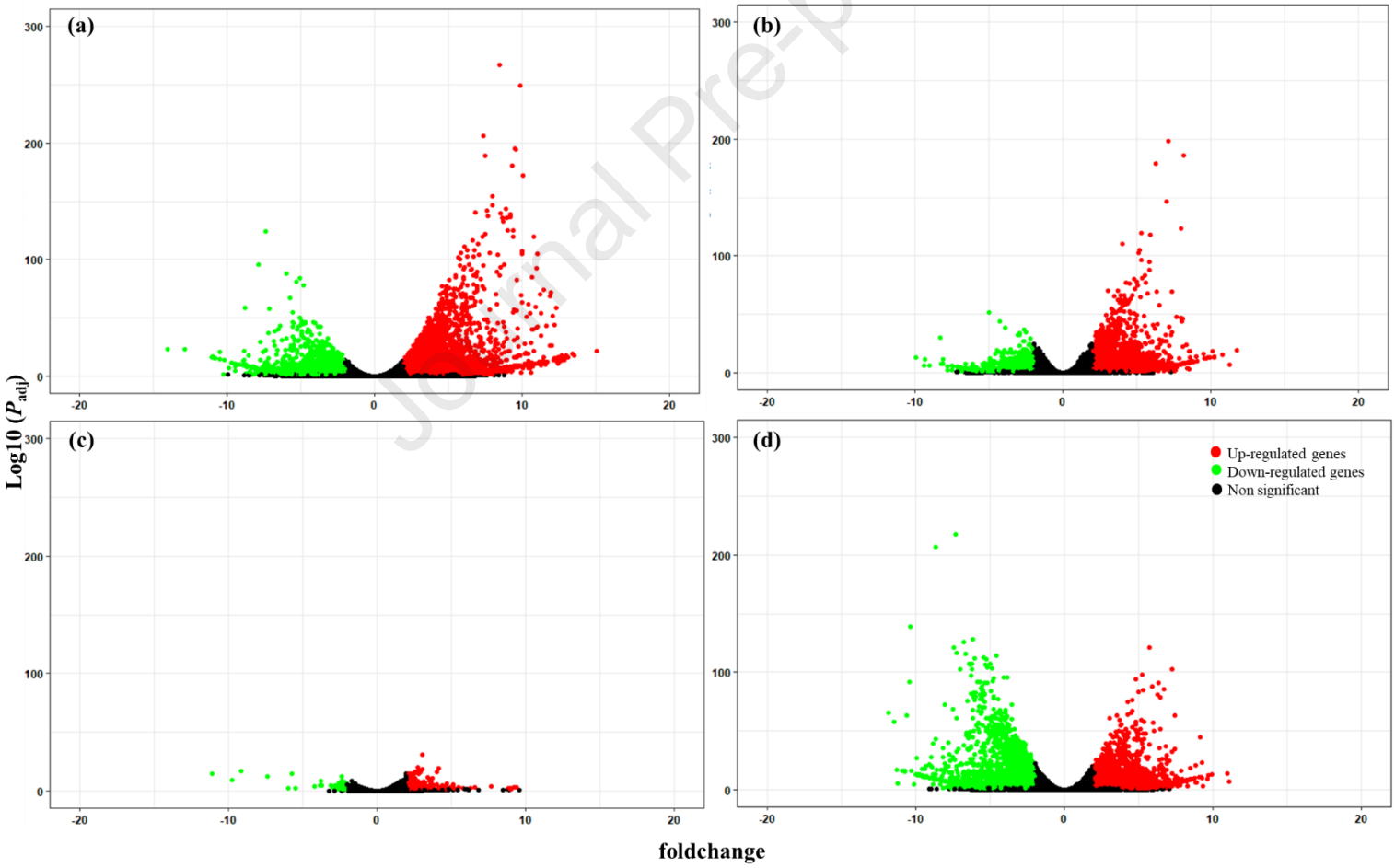


**Fig. 6** Volcano plots of differentially expressed genes identified in callus of *C.* x *powellii* "Album" (a) 2 mg/L of 2,4-D: Light Vs Dark , (b) 4 mg/L of 2,4-D: Light Vs Dark, (c) Dark: 4 mg/L Vs 2 mg/L of 2,4-D and (d) Light: 4 mg/l Vs 2 mg/L of 2,4-D. Differential expression analysis was performed using the R package DESeq2. p-values

were adjusted for controlling the false discovery rate (FDR). Only genes with $|\log_2(\text{FoldChange})| > 2$ and an adjusted p-value < 0.05 were considered as significant differentially expressed. Red indicates up-regulated genes, green indicates down-regulated genes, and black indicate genes non-significant deregulated genes.

Supporting the principal component analysis result, differential expression analysis showed that the exposure to light had a greater impact on gene expression than did the concentration of 2,4-D (Fig. 6). A total of 11,304 and 4505 genes were deregulated in light vs dark condition with exogenous supply of 2 or 4 mg/L of 2,4-D, respectively (Fig. 6a, 6b ; Fig. 7a). GO enrichment analysis showed that genes involved in, "tetrapyrrole binding", "monooxygenase activity", "oxidoreductase activity" and "response to stimulus" were up-regulated in light condition regardless of concentration of 2,4-D supplied. "Photosynthetic membrane " and "photosystem" related transcripts were up-regulated in light vs dark condition at 2, and 4 mg/L of 2,4-D, respectively. The 3401 genes up-regulated in callus grown with 4 mg/L of 2,4-D exposed to light were enriched in the "phenylpropanoid metabolic process", whereas the "phenylpropanoid catabolic process" was downregulated (Fig. 7a).

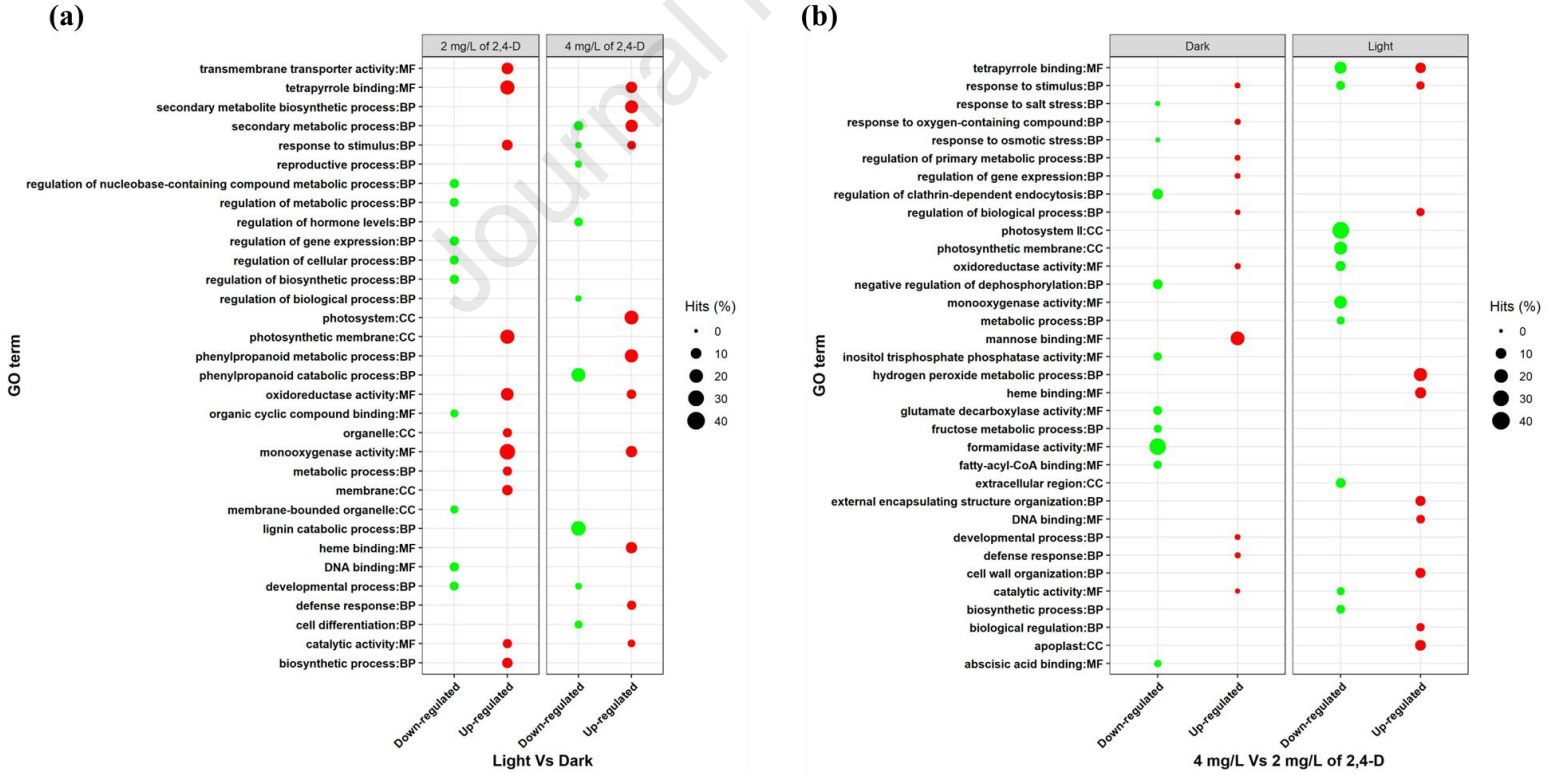


**Fig. 7** Gene Ontology analysis of differentially deregulated genes. (a). Comparison of differentially expressed genes in calli developed with in light Vs dark with supply of 2 mg/L or 4 mg/L of 2,4-D. (b). Comparison of differentially expressed genes in calli developed in 4 mg/L Vs 2 mg/L of 2,4-D in light or dark condition. Red and green colours

indicate the down regulated and upregulated genes, respectively. Analysis was done with a *p*-value of 0.05. Y-axis in each figure represent the GO term and ontology (MF: molecular function, BP: Biological process, CC: cellular component).

To understand the effect of 2,4-D on *C.* x *powellii* "Album" callus transcriptome, we also performed differential gene expression analysis between calli obtained using 4 mg/L compared to 2 mg/L of 2,4-D, with and without light exposure (Fig. 6c, 6d; Fig. 7b). In light condition, 4 936 genes were up-regulated, and 4 129 gene were down-regulated in culture with 4 compared to 2 mg/L of 2,4-D (Fig. 6d; Fig. S7a). Compared to samples exposed to light, a smaller number of genes were differentially expressed between, with only 455 genes deregulated in dark conditions, consistent with the PCA result (Fig. S6). When grown with 4 mg/L of 2,4-D in darkness, genes involved in "oxidoreductase activity", "defense response" and "developmental process" were up-regulated compared to the lower concentration of 2,4-D, whereas genes involved in "formamidase activity" was the most commonly down-regulated GO-category. The most enriched category among the up-regulated genes in 4 vs 2 mg/L of 2,4-D exposed to light, was the "hydrogen peroxidase metabolic process" and "tetarpyrolle binding", whereas down-regulated genes were observed in "photosystem II", "oxidoreductase activity" and "monoxygenease activity".

### 2.8 2,4-D and light affect the expression pattern of genes involved in phenylpropanoid and AA biosynthesis

Candidate AA biosynthetic genes, from the precursor shikimate pathway to AA specific genes, were identified in *C.* x *powellii* "Album" transcriptome on the basis of Blast homology searches. We identified a total of 78 complete and partial hits to genes that are putatively involved in the shikimate, the phenylpropanoid and the AA pathways and their corresponding gene transcript sequences were deposited in GenBank with the accession numbers listed in Table S5. Candidate genes involved in the AAs biosynthesis were selected based on homology and on their differential expression profile, *i.e.* only the genes that were upregulated in conditions that accumulated AAs were selected. Overall, there was significantly more transcripts in light (with 2 or 4 mg/L 2.-4D) compared to dark condition, when callus cultures were treated with 2 ($p<0.001$ and $p=0.002$, respectively, Friedman multiple comparisons test, Fig. S8) or 4 mg/L of 2,4-D ($p=0.0102$ in both cases). Specifically, light and 2,4-D both impacted specifically on the gene expression profile of *CpPAL*, *CpTYDC*, *CpC3H*, *CpHCT*, *CpOMT*, *CpNBS*, *CpNR*, *CpCYP96 and CpV11H* (Table S5; Fig. S8). On the right arm of the AAs precursors biosynthetic pathway that leads to 3,4-DHBA

(Fig. 1), the exposure of callus to light led to a 3.35 to 4.55 $log_2$ fold increase in expression of *PAL (i.e. CpPAL1)* compared to callus grown in the dark. In this condition, candidate genes involved in the phenylpropanoid pathway, such as *CpC4H, CpC3H, Cp4CL, and CpHCT1* were also up-regulated (Table S5, Fig S8a.). On the left arm of AA precursors pathway leading to tyramine (Fig. 1), *CpTYDC1* candidate followed a very similar profile to *CpPAL1*, greatly up-regulated by light, but also by 2,4-D concentration (Fig S8a). *CpNBS* transcripts, encoding the enzyme predicted to be involved in the condensation of 3,4-DHBA and tyramine to give norbelladine, was expressed at very low levels overall, and upregulated in callus exposed to light and 4 mg/L of 2,4-D compared to dark condition (Table S5, Fig S8b). Furthermore, a 6.07 $log_2$ fold increase was observed for *CpNBS* in light condition with supply of 2 mg/L of 2,4-D. A candidate gene homologous of the norbelladine *O*-methyltransferase (*CpN4OMT*) was upregulated by a 2.67 $log_2$ fold in light compared to dark condition when supplied with 4 mg/L of 2,4-D. Interestingly, although the gene encoding a cytochrome p450 monooxygenase enzyme homologous to *CYP96T*, responsible for the phenol-phenol coupling of 4-*O*-methylnorbelladine, was expressed at low level overall, but mostly expressed in callus exposed to light (a 2.48 to 5.52 $log_2$ fold increase compared to dark), its expression was lower in 4 mg/L compared to 2 mg/L of 2,4-D in light conditions.

Furthermore, to understand the effect of photosynthesis-related and auxin inducible genes, we performed a WGCNA analysis. From 12526 DEGs, 1092 genes with a raw count > 10 were selected for WGCNA analysis, leading to the identification of seven modules, indicated by different colors (Fig. 8; Fig. S9). Among all modules, turquoise included the highest number of genes (403 genes) while the red module contained only 30 genes (Fig. 8). Candidate genes of AAs and phenylpropanoid biosynthesis pathways all clustered in the turquoise module, suggesting that these two pathways are interconnected. In this module that was selected for further analysis,185 genes were significantly correlated (Spearman correlation > 0.8). We identified 9 transcription factors (i.e. B-box zinc finger protein 24 (BBX24),NAC domain containing protein (NAC58 and NAC83), Homeobox-leucine zipper protein (HOX21), transcription factor MYB78, WRKY transcription factor (WRKY24 and WRKY75),Zinc-finger transcription factor( ZAT12), 3 genes encoding auxin inducible proteins (*i.e* (auxin responsive protein (ARFG), two SUR32 (auxin responsive protein)), and 4 genes encoding f photosynthesis related proteins (i.e. SGR protein STAY-GREEN homolog(SGR),photosystem II stability/ assembly factor HCF136 (P2SAF,Chromoplast-specific carotenoid-associated protein C1 (CHRC1)and Chorophyll a-b

binding protein (CB2D, together with genes involved in phenylpropanoid and AAs pathway. These results show that auxin-inducible genes and photosynthesis-related genes are interconnected with specialized metabolites biosynthesis gene.

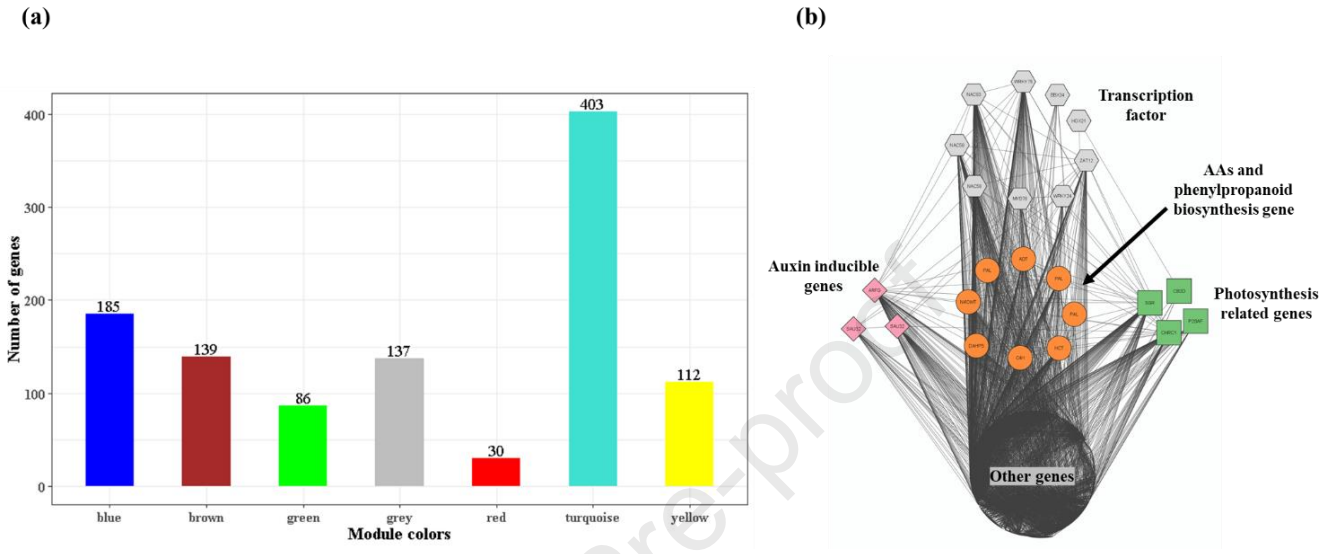


**Fig. 8** Weighted gene co-expression network analysis (WGCNA) of differentially expressed genes (DEGs) identified from four culture conditions. (a) Bar graph showing number of genes present in seven identified modules, which are shown in designated colors: “Blue”, “Brown”, “Greens”, “Grey”, “Red”, “Turquoise” and “Yellow”. The bar graph color of bar graph corresponds to the hierarchical cluster tree in Fig S9.b, each color specific to a module. (b) Co-expression network analysis of genes involved in phenylpropanoid & AAs biosynthesis (orange, circular), auxin-inducible genes (pink, lozenge), transcription factors (grey, hexagonal), photosynthesis related genes (green, rectangular) and other genes present in modules turquoise. For network analysis, gene having Spearman correlation > 0.8 and p-value < 0.05 were selected from the turquoise module.

## 3. Discussion

To boost the production of specialized metabolites *in planta* or in heterologous hosts, it is essential to uncover the conditions that trigger their production and to understand their biosynthetic route. Accumulation of AAs is affected by the type of tissue, and both, biotic and abiotic stresses. For example, light exposure affects growth and development, as well as the synthesis and accumulation of specialized metabolites in plants, as shown in studies in *Leucojum aestivum* L. and *Lycoris longituba* (Li et al., 2021; Moranska et al., 2023). In addition, phytohormones play a critical role in tissue differentiation and growth. Auxins promote cell elongation and control a variety of functions, including organogenesis, general shoot and root architecture, responses to light and gravity, and tropic growth (Khadr et al., 2020; Ptak et al., 2013; Woodward and Bartel, 2005). Recently, the effect of different levels of NAA on the tissue differentiation of *Narcissus pseudonarcissus* cv. Carlton was reported, and it was shown that the synthesis and accumulation of AAs vary with the type of tissue (Ferdausi et al., 2020). Indeed, these factors are easily manipulated in *in vitro* cultures, which also enable the fine-tuning of alkaloid production and related gene expression analysis (Gallego et al., 2018). Complementarily, comparative transcriptomics and targeted metabolomics studies of *in vitro* cultures can uncover genes associated with biosynthesis of specific metabolites of interest (Kilgore et al., 2014; Singh and Desgagne-Penix, 2017; Wang et al., 2016). Because AAs profile is usually less diversified than *in planta, in vitro* cultures have the advantage to provide a template with a more focused pathway and less background noise. Therefore, as first aim in this study, we developed *in vitro* tissue culture to study the effect of light and auxin and to understand the AAs biosynthetic route in *C.* x *powellii* "Album" at both, the metabolomic and the transcriptomic levels.

*C.* x *powellii* "Album" shows a close relationship with the South-African clade of *Crinum* species, including *C. bulbispermum, C. stuhlmannii* and *C. moorei*. This phylogenetic analysis is consistent with the known origin of *C.* x *powellii* "Album" as a crossing between *C. bulbispermum* (orange river lily) and *C. moorei* (natal lily) (Meerow et al., 2003). GC-MS analysis revealed that *C.* x *powellii* "Album" methanolic extracts contained lycorine, cherylline and crinine ,as reported previously (Nino et al., 2007; Velten et al., 1998), together with additional AAs. The detection of AAs of lycorine- and crinine-types suggests that AA biosynthesis in *C.* x *powellii* "Album" follows mainly two types of phenol-oxidative coupling of 4'-*O*-methylnorbelladine, *i.e*. 'para-para' and 'ortho-para' (Fig. 1). Indeed, AAs that follow para-ortho' coupling reactions, such as

galanthamine, were not detected. Interestingly, cherylline, an AA more specifically isolated from *Crinum* species, was detected in all tissues except in leaves extract, suggesting that either cherylline biosynthesis does not occur in this tissue, or it may transfer to and accumulate in other parts of plant.

Since bulbs of *C.* x *powellii* "Album" contained all three ring-types of alkaloids, it was selected as an explant source for tissue culture, starting from twin scale extracted from its inner part, as previously reported (Aleya et al., 2021; Priyadharshini et al., 2020; Slabbert et al., 1993; Trujillo-Chacon et al., 2020). The major challenge associated with the development of *in vitro* culture from explants, such as bulbs, is the presence of endophytic contamination. Although disinfection of Amaryllidaceae (*Zephyranthes grandiflora* and *N. tazetta* L.) bulbs has been performed using mercury chloride, this compound is excessively toxic. Here, we performed a heat treatment at 52°C for one hour, followed by ethanol washing and bleach treatment, and no contamination was detected following the initiation of *in vitro* culture. This indicated that our surface sterilization methodology was effective to remove endophytic microorganisms from the explant, in agreement with other reports (Ferdausi et al., 2020; Langens-Gerrits et al., 1998; Xu et al., 2020). Another common challenge associated with *in vitro* culture of plants is explant browning, which occurs mainly due to accumulation and oxidation of phenolic compounds (Dixon and Paiva, 1995; Ndakidemi et al., 2014). Plants produce phenolic compounds in response to stress, such as wounding and changes in culture environment, commonly occurring during the extraction of explant and *in vitro* culture of plant tissues. In our study, browning was specifically observed in callus exposed to light and higher concentration of 2,4-D, which indicated that these conditions may be toxic for newly developing tissue. Previous reports on parental *C. moorei in vitro* culture also showed a higher ratio of explant browning in light condition (Fennell et al., 2003). Following successful initiation of *in vitro* culture and survival, explants may develop into different tissue. The type of auxin supplied in the culture media impacted the type of tissue generated, and auxin addition was necessary to induce callus, conforming to previous reports (Rahimi Khonakdari et al., 2020). In the presence of 2,4-D, explants grew as undifferentiated tissue, regardless of its concentration and exposure to light. For light exposed callus supplemented with 2 or 4 mg/L of NAA, shoot generation occurred within 8 weeks, whereas with 8 mg/L NAA, 14 weeks were necessary for tissue differentiation. For callus that were not exposed to light, tissue differentiation arose on the $10^{th}$ week of culture when supplied with 2 or 4 mg/L of NAA, however no shoot

formation was seen with higher concentrations of NAA, in agreement with other studies on *N. pseudonarcissus* cv. Carlton tissue (Ferdausi et al., 2020). Our results show that exogenous supply of auxin and light modulate tissue differentiation during *in vitro* culture of *C.* x *powellii* "Album".

Second, we explored the metabolite profiles of different types of tissues developed during *in vitro* culture using GC-MS and LC-MS/MS. The accumulation of AAs was higher in in differentiated tissues as compared to callus, which probably relates to organ-specific biosynthesis of AAs, as reported in *L. aestivum* L. and *C. moorei*, or to the involvement of multiple tissues in AAs biosynthesis (Demir et al., 2022; Elgorashi et al., 2002). Furthermore, tissue exposed to light stress were also actively involved in photosynthesis, ,providing access to higher carbon source, which could result in higher AAs accumulation in light condition (Aleya et al., 2021; Rahimi Khonakdari et al., 2020). Detection of crinamidine, a crinine-type of AAs was surprising, as they were not detected in *in vivo* samples of *C.* x *powellii* "Album" This might indicate that metabolites analysis of native plant may not always be sufficient to reveal its SMs biosynthesis potential. Moreover, plant produce SMs as defensive response to biotic and abiotic response, therefore biosynthesis of SMs such as crinamidine could be related to plant defense response. This suggests that harsh culture condition can be utilized to induce SMs biosynthesis. Furthermore, mature plant organs often maintain their relative cell undifferentiated stage to adjust to different hormonal changes and stress (Ikeuchi et al., 2015). Cellular differentiation results in global changes of gene expression patterns, including SMs biosynthesis genes, which is probably related to higher alkaloid content in differentiated tissue as compared to undifferentiated tissue, but also to differential alkaloid profile in newly growing *in vitro* tissue as compared to mature *in vivo* tissue (Bruex et al., 2012; Taylor-Teeples et al., 2015). ,. AAs profile in callus was also distinct between the culture condition (light) and between the type and the concentration of the hormone used. SMs, including phenylpropanoids and AAs, accumulated at higher levels in the light condition compared to dark, regardless of the type of auxin that was used, in keeping with reports in *Agastache rugosa* (Korean mint) (Park et al., 2020), and in Amaryllidaceae *L. aestivum* L. and *L. longituba* (Li et al., 2021; Moranska et al., 2023). These results show that *in vitro* tissues of *C.* x *powellii* "Album" conserved a biosynthetic capability that can be manipulated by modifying the culture conditions. The expression of genes encoding biosynthetic enzymes are often regulated by chromatin remodeling which is indeed related to the level of cell differentiation (Ikeuchi et al., 2015). Another important factor that can regulate differential alkaloid biosynthesis in different types of tissue is RNA post-

modification such alternative splicing of genes (Lam et al., 2022). However, we observed low abundance of transcript belonging to "RNA processing and modification" as well as "chromatin structure and dynamics" in our assembled transcriptome. These processes, when measured at the proteomic levels, have been associated with increased accumulation of Amaryllidaceae alkaloids, although the mechanism is not known (Tang et al., 2023). Even though, callus produced fewer types of alkaloids, they were responsive to light and 2,4-D, and so could provide a straightforward matrix to resolve the biosynthetic route of specific AAs as compared to RNA-seq data generated from *in vivo* tissues. Hence, the calli were selected as homogenous biological sample for transcriptomic study. Genes related to photosynthesis and involved in tetrapyrrole binding activity were up-regulated in calli exposed to light, regardless of 2,4-D concentration. Increased activity of tetrapyrrole binding helps the plant to adapt under different stress conditions, including excess or lack of light. Oxidoreductase activity and monooxygenase activity were also enriched GO term categories in the light condition. When calli were grown in absence of light, genes related to mannose binding, crucial for plant defense signaling during pathogen attack, were upregulated by increased concentration of 2,4-D (Hwang and Hwang, 2011; Ma et al., 2023). We did not observe any contamination during this study, and to our knowledge, there is no data associating 2,4-D concentration with mannose binding gene expression. This was intriguing, as phenylpropanoids and alkaloids, which are also produced to defend the plant against external stress, accumulated as well in these conditions.

Next, based on homology search, we identified candidate gene transcripts including *TYDC*, *PAL*, *C4H*, *C3H*, *4CL*, *HCT*, *NBS*, *OMT*, *CYP96T*, *NorRed*, and *V11H*, which are putatively involved in the phenylpropanoid and AA biosynthetic pathways (Fig. 1). High % (>75%) of amino acid sequence identity with functionally characterized homologous gene from other Amaryllidaceae plants strongly suggests that these gene transcripts encode enzymes involved AA metabolism. However, the biosynthetic route of several AAs, such as methylated norbelladine, is still unknown (Desgagné-Penix, 2020; Koirala et al., 2022).We identified CYP96T transcript sequences in the transcriptome of *C.* x *powellii* "Album" together with alkaloids resulting from different phenol-phenol coupling reactions, suggesting that they may be involved in the proposed reactions (Kilgore et al., 2016). Further AAs biosynthesis gene mining from *C. x powelllii* "Album" transcriptome, and their functional characterization will provide a solid understanding of AAs biosynthesis type. Interestingly, the transcript sequences encoding the first step of each part of the 'divided' pathway

(*CpPAL1, CpTYDC1, CpNBS, CpCYP96T*) were all accumulating at lower levels compared to the others transcripts involved in the pathway (Fig. S8). This suggests a possible high-point of regulation of the first committed step regulating the entry of metabolites. Furthermore, each of these transcripts were up-regulated in the same conditions (light and 2-4D) suggesting that these biosynthetic pathways are coordinately regulated. Overall, the expression level of candidate transcripts were higher in calli exposed to light compared to those grown in the dark, and was also modulated by 2,4-D addition. Thus, light and auxins led to an increase in AAs and AA precursors at both metabolomic and transcriptomic levels. This is probably related to their protective role from the damages caused by light (Wink, 2008; Winkel-Shirley, 2001). In conditions of light exposure, an increased concentration of 2,4-D led to a decrease in photosynthesis related genes, and an accumulation of transcripts associated with hydrogen peroxide catabolic process and with the apoplast. These genes are related to cell death, indicating that 4 mg/L of 2,4-D in calli exposed to light may be toxic and trigger programmed cell death (Gupta et al., 2016; Yoda et al., 2003), in accordance with the observed lower survival of explants and with El Tahchy et al. (2011). Alternatively, alkaloid accumulation triggered by light and 2,4-D could be the cause of this toxicity. Indeed, the expression levels of genes related to production of phenylpropanoid compounds, and AA biosynthetic pathways are interconnected with each other, together with photosynthesis-related and hormone-induced genes, linking light and auxin response to their expression. Refining the equilibrium between stress and death appears to be key to optimize alkaloid production.

## 4. Conclusion

As an alternative to native plant sources, biotechnological approaches have been developed to increase the production of plant biomass and yield a sustainable supply of plant-derived compounds, essential to fully explore their biological potential and use them as therapeutic agents (Koirala et al., 2022; Priyadharshini et al., 2020; Tallini et al., 2018). In this study, we developed *in vitro* cultures of *C.* x *powellii* "Album" with 2,4-D and NAA at three different concentrations, exposed or not to light. We showed that exogenous supply of auxin is necessary for callus induction in *C.* x *powellii* "Album". 2,4-D at 2 mg/L efficiently induces callus formation in this species, whereas different concentrations of NAA promote shoot formation. We detected more AAs in tissues exposed to light compared to those grown in dark, while accumulation of AAs was higher in differentiated tissues. Indeed, light condition promoted the synthesis and accumulation

of alkaloids, and differentiated tissues are more suitable for AAs production from *C* x *powellii* "Album". Consistently, transcriptomic studies showed that genes related to stress are upregulated in callus exposed to light, associating the production of SMs to a protection mechanism against light in *C.* x *powellii* "Album". With optimal selection of growth hormone and culture conditions, *in vitro* tissues can potentially be exploited for the production of AAs in *C.* x *powellii* "Album", including cherylline. The differential transcriptomic data obtained in this study also paves the way to the discovery of cherylline and lycorine pathways, required to bioengineer heterologous microbial hosts to produce these potent molecules.

## 5. Experimental

### 5.1 Plant material and chemical reagent

*C.* x *powellii* "Album" bulbs (Fig. 2a) were purchased from commercial market (Phoenix perennials, Canada). Plant growth hormones (2,4-dichlorophenoxyacetic acid (2,4-D), 6-benzylaminopurine (BAP), kinetin, Phytagel, sucrose and plant preservative mixture (PPM) were all purchased from Millipore Sigma (Massachusetts, USA). Murashige and Skoog (MS) medium was from PhytoTech Labs (Kansas, USA). Standards of the alkaloids 11-hydroxyvittatine, 9-O-demethylhomolycorine, cherylline, flexinine, gigancrinine, gigantelline, gigantellinine, haemanthamine, homolycorine, obliquine, pancracine, sanguinine, tazzetine, vittatine and crinine were kindly obtained from Professors Antonio Evidente and Marco Masi (Universitario Monte Sant'Angelo, Naples, Italy). Standards of 3ˈ-*O*-methylnorbelladine, 4ˈ-*O*-methylnorbelladine, 3ˈ4ˈ-*O*-dimethylnorbelladine and norbelladine were synthetized as described in (Girard et al., 2022). Standards of 3,4-dihydroxybenzaldehyde (97%), 4-hydroxybenzaldehyde (99%), isovanillic acid (99%), isovanillin (98%) and *trans*-cinnamic acid (98%) were purchased from Acros Organics (Massachusetts, USA). Standards of 3,4-dihydroxybenzoic acid (97%), levodopa (98%), L-tyrosine (99%) and *p*-coumaric acid (98%) were purchased from Alfa Aesar (Massachusetts, USA). Standards of caffeic acid (98%), dopamine (98%), ferulic acid (99%), lycorine (98%), papaverine (98%), tyramine (99%) and vanillin (99%) were procured from Millipore Sigma (Massachusetts, USA). Standards of galanthamine (98%) and narciclasine (98%) were purchased from Tocris Bioscience (Bristol, United Kingdom). Standards of norgalanthamine, lycoramine (97%), coclaurine (95%), isoferulic acid (98%), and phenylalanine 98%) were obtained from Toronto Research Chemicals (Ontario, Canada), US Biological, Musechem (New

Jersey, USA), TCI America (Oregon, USA), and MP Biomedicals (California, USA) respectively. Analytical LC-MS grade methanol was purchased from Fisher scientific (New Hampshire, USA)

### 5.2 Genotyping of plant samples

To determine the genotype of the plant sample, total genomic DNA was extracted by using the plant DNA extraction mini kit (Qiagen, Hilden, Germany), according to the manufacturer's protocol, and the quality of genomic DNA was estimated by using Implen nanophotometer (California, United states). Highly conserved internal transcribed spacer 2 (*ITS2*) region were amplified using gene-specific primers (i.e forward primer 5'-ATGCGATACTTGATGTGTGAAT -3' and reverse primer 5'-GACGCTTCTTCTCCAGACTACAAT-3') ), with Q5 DNA polymerase (New England Biolab, Massachusetts, USA). The specificity of the amplified region was verified following agarose gel electrophoresis and sequenced using Sanger sequencing at Genome Quebec Innovation Centre (QC, Canada). Phylogenetic analysis was performed by using Neighbor-Joining method in Mega11 software, including *ITS2* regions from 10 *Crinum* species. *Amaryllis belladonna* (Amaryllidaceae family) was used as outgroup(Saitou and Nei, 1987; Tamura et al., 2021).

### 5.3 Development of *in vitro* culture

Two bulbs of *C.* x *powellii* "Album"of approximately 75 grams were selected and surface sterilized according to Ferdausi *et al.* 2020, with some modifications (Ferdausi et al., 2020). Briefly, *C.* x *powellii* "Album" bulbs were kept at 4℃ for 4 weeks, and then at room temperature for 24 hours. Leaves, roots, and bulbs were separately flash frozen in liquid nitrogen and kept at -80℃ for further alkaloid analysis. Bulbs underwent a heat treatment at 52℃ for 1 hour and were then kept at room temperature overnight. For surface sterilization, dead and dry scales were removed before bulbs were washed with tap water and detergent five times and dipped into 70% ethanol for 1 minute. Then, bulbs were treated for 30 minutes with commercial bleach containing 6% of sodium hypochlorite. Afterwards, bulbs were washed with autoclaved water five times inside a biological hood. Several layers of bulb scales were removed to reach the inner part of the bulbs. Finally, ~100-120 twin-scale size explants were obtained from each bulb. Untreated bulb, surface sterilized bulb, and example of a twin scale explants are shown in Fig. S1.

Basic media was prepared with MS supplemented with 3% of sucrose, 0.075% of PPM, 3 g/L of Phytagel, 0.5 mg/L of BAP, 0.5 mg/L of kinetin and 100 mg/L of yeast extract. The pH was

adjusted to 5.7 ± 0.1 before adding phytagel and autoclaving. Plant growth hormones were added after sterilization. This basic media was used as a control to measure the effect of auxin in *C.* x *powellii* "Album" *in vitro* culture. During the experiment, two different types of auxins, *i.e.*, 2,4-D and NAA, were used at three concentrations, *i.e.*, 2, 4, and 8 mg/L. Five explants were cultured in each plate at 23°C in light conditions (14hs:10hs light:dark, 100 µMol/$m^2$) or in 24h dark conditions. Explants were sub-cultured every two weeks. Then, the effects of light and auxin on explant's characteristics were recorded. To generate enough sample material, culture was continued for 6 months.

**5.4 Metabolites extraction**

Different types of tissues from native plant (young leaves, bulbs, basal plates and roots) and from *in vitro* culture tissue, *i.e.*, callus and differentiated tissues, were selected for alkaloid analysis. Samples were grounded into a fine powder upon addition of liquid nitrogen using a pestle and mortar. Then, crude alkaloids were extracted with 1 mL of methanol per 100 mg of plant sample with continued shaking for 24 hs, followed by sonication for 30 min at room temperature. Extracts were centrifuged at 5000 g for 10 min, and supernatants were transferred into a new falcon tube and completely evaporated using Thermo Scientific Savant SPD1010 SpeedVac Concentrator (Massachusetts, USA). Samples were resuspended in LC-MS/MS grade methanol (100 µL per 100 mg of the initial sample) by sonication, then centrifugated at 10 000g for 10 min and filtered through 0.22 µM nylon filter.

**5.5 Metabolites constituents analysis by GC-MS**

For GC-MS analysis, *in vivo* tissues and *in vitro* samples were resuspended in LC-MS/MS grade methanol (100 µL per 100 mg of initial sample) and were directly injected into the GC-MS (Agilent Technologies 6890N GC coupled with 5973N inert MSD) in EI (Electron Ionization) mode at 70 eV. The temperature ramp was done as follows: temperature was set at 100°C for 2 min, followed by 100–180°C at 15°C $min^{-1}$, 180–300°C at 5°C $min^{-1}$, and a 10 min hold at 300°C. Injector and detector temperatures were set at 250°C and 280°C, respectively, and the flow rate of carrier gas (He) was 1 $mL.min^{-1}$. The GC column was an Agilent J&W DB-5Ms Ultra Inert Column (30 m x 0.25 mm x 0.25 µM, Agilent technology, Santa Clara, USA). A split ratio of 1:10 was applied, and the injection volume was 1 µL. Alkaloids were identified by comparison with the 2005 National Institute of Standards (NIST) database based on matching mass spectra, GC-MS

spectra of authentic compounds previously isolated and identified by other spectroscopic methods in these species, or with data obtained from the literature. All raw GC-MS experimental data were deposited in MetaboLights database (http://www.ebi.ac.uk/metabolights) (accession number: MTBLS8511) (Haug et al., 2020).

### 5.6 Targeted metabolite analysis by LC-MS/MS

Targeted metabolite analysis for AAs precursor molecules and AAs were performed on *in vitro* tissue. A high-performance liquid chromatography (HPLC) coupled with a tandem mass spectrometer (MS/MS) (Agilent, QC, Canada) equipped with an Agilent Jet Stream ionization source, a Kinetex EVO C18 column (150 x 4.6 mm, 5 μm, 100 Å; Phenomenex, Torrance, USA), a binary pump, an autosampler set at 4°C and a column compartment were used for the analyses. Five μl of each sample were injected into the column that was set at 30°C. A gradient made of (A) formic acid 0.1% v/v in milli-Q water and (B) methanol, with a flow rate of 0.4 mL/min, was used to achieve chromatographic separation. The HPLC elution program started with 10% solvent B; 0-10 min, isocratic conditions with 10% B; 10-20 min, linear gradient to reach 100% B; 20-25 min, isocratic conditions with 100% B; 25-26 min, linear gradient to return to initial conditions of 10% B. The total run time was 30 min per sample to allow the reconditioning of the column prior to the next injection. The parameters used for the MS/MS source to perform the analyses were set as follows: gas flow rate 10 L/min, gas temperature 300°C, nebulizer 45 psi, sheath gas flow 11 L/min, sheath gas temperature 300°C, capillary voltage 4000 V in ESI+ and 3500 V in ESI– and nozzle voltage 500 V. Agilent MassHunter Data Acquisition (version 1.2) was used to control the HPLC-MS/MS, MassHunter Qualitative Analysis (version 10.0) and MassHunter Quantitative QQQ Analysis (version 10.0) were used for data processing. MRM transitions and instrument parameters used in ESI+ for identification of target compound during LC-MS/MS analysis are included in Table S2.

### 5.7 Total RNA extraction, *de novo* transcriptomic assembly, and functional annotation

Total RNA was extracted from different plant organs (roots, bulbs, basal plate, and leaves) and from *in vitro* tissues (callus developed with 2 mg/L and 4 mg/L of 2,4-D in light and dark conditions). For *in vitro* tissues, RNA was extracted by using a Qiagen RNeasy Plant Mini kit (Hildon, Germany), using approximately 100 mg callus samples according to the manufacturer's protocol. For *in vivo* tissues, total RNA was extracted using the method described in Meisel et al.

(2005). Briefly, 1 g (fresh weight) of *in vivo* tissues were homogenized and the powder was transferred to a tube containing 5 mL of extraction buffer (20 mg/ml CTAB,100 mM of Tris-HCL pH 8, 20 mM EDTA, 1.4 M NaCl, 10 mg/ml of polyvinylpyrrodine, 100 µL of β-mercaptoethanol and 50 µl of spermidine trihydrochloride) at 65 °C. After agitation, extraction of nucleic acids was performed twice with chloroform:isoamyl alcohol 24:1. RNA was precipitated overnight with 0.25x of 10M LiCl at 4ºC. After centrifugation at 12 000 g for 35 min at room temperature, the pellet was resuspended in 0.5 mL of DEPC-treated $H_2O$. Another extraction was performed with chloroform:isoamyl alcohol 24:1, and after centrifugation at 14 000g for 30 min at 4ºC, RNA was precipitated in the aqueous phase by adding 1 mL of 100% ice cold ethanol and incubating for 30 min at -80ºC. After centrifugation at 14 000 g for 20 min at 4ºC, the pellet was washed with 1 mL of 75% ethanol. Finally, RNA pellet was resuspended in 50 µL of DEPC-treated $H_2O$. Three independent biological replicates from each sample type were used for transcriptomic analysis, except for callus obtained in dark conditions with 2 mg/L of 2,4-D (n=2), for which one sample was rejected due to low RNA quality.

The mRNA was converted into a cDNA library and sequenced through Illumina NovaSeq 6000, sequencing system, with paired-end reads of 100bp, at Genome Quebec Innovation Centre (Montreal, QC, Canada). Raw reads were analyzed using FastQC (v0.11.9) for quality control (Conesa et al., 2016) and visualized with MultiQC (v1.13). The quality trimming was performed using modified Fastp (v0.23.1) software with cut front mean quality 20, cut tail mean quality 20 and length required 50. Then *de novo* transcriptomic assembly of all the generated clean reads was performed with Trinity assembler (v2.14.0) using default parameters. The completeness of the transcriptome assembly was assessed with BUSCO (v5.2.2) using embryophyte_odb_10. The coding regions were predicted using TransDecoder (version 5.5.0) (http://transdecoder.github.io/). The longest open reading frames (ORFs) obtained were functionally annotated with Trinotate pipeline (version 2.0) (http://trinotate.github.io/) (Bryant et al., 2017). Briefly, the assembled *C.* x *powellii* "Album" transcriptome was searched against the UniProt database (release 2022_04) using blastp and blastx (blast+ v2.12.0) with e-value threshold of 1e-5 to identify homologous proteins. Putative signal peptides were predicted with SignalP (v4.1) and conserved protein domains were identified with HMMER (v3.3.2) using Pfam-A database (v3.1b2). The gene ontology (GO) of the annotated transcripts was extracted to illustrate the ten most abundant GO terms of each category (molecular function, cellular component, and biological process). Assigned Clusters of

Orthologous Genes (COGs) id was used to identify the COG annotation using cog-20 and fun-20 (https://ftp.ncbi.nih.gov/pub/COG/COG2020/data)(Galperin et al., 2021). Candidates annotated gene transcript sequences were deposited in GenBank with the accession numbers listed in Table S5 (supplementary excel file).

### 5.8 Differential gene expression analysis, putative Amaryllidaceae alkaloids gene identification and co-expression analysis

Clean reads were aligned to the assembled transcriptome, and the read count per gene was determined for each sample using RSEM software v1.3.3 (Li and Dewey, 2011). The raw read counts per gene was used to analyse differential expression with the R (4.2.2) package DESeq2 (Anders and Huber, 2012) using default parameters and genes $|\log_2(\text{fold change})| > 2$ at an adjusted p-value $\leq 0.05$ were considered as significantly deregulated. Gene ontology enrichment analysis was further performed on differentially expressed genes (DEGs) sets.

To identify the putative genes encoding the enzymes involved in the phenylpropanoid pathways, and AAs pathways local blast search was performed. Local Blastx was performed by using from assemble transcriptome data of *C.* x *powellii* "Album" and characterised genes were used as query with blast+ version 2.13.0.

Furthermore, to understand the expression pattern of genes related to phenylpropanoid and AAs pathways, and with auxin photosynthesis, Highly co-expressed gene modules were inferred from the DEGs generated with *in vitro* and *in vivo* tissue samples using the R package WGCNA (Langfelder and Horvath, 2008).. Prior to the WGCNA analysis, selected gene sets were filtered for outlier samples and for raw count value greater than 10 in 50% of sample. The soft thresholding power β of 14 was selected to make the networks exhibit an approximate scale-free topology (Fig. S7a). Co-expression modules were identified using the blockwiseModules function and the Dynamic Tree Cut algorithm with minimum module size 30, a branch merge cut-off height of 0.25 and "signed" TOMtypes (Zhan et al., 2015). All genes were hierarchically clustered based on TOMsimilarity, and a gene dendrogram was produced. The module that encompassed phenylpropanoid and AAs biosynthesis genes was selected for further analysis. Spearman correlation was calculated for each pair of genes present in the module of interest. Genes having correlation > 0.8 with *p*-value 0.05 were selected for network visualization by Cytoscape 3.9.1. Genes were annotated as auxin inducible genes, photosynthesis related genes and transcription

685 factors on the basis trinotate file generated during this study.Finally, GraphPad Prism v10.0.2
686 (GraphPad software LLC) was used to generate Fig. 5, Fig. S4 Fig. S8 and the associated statistics.

687

## 6. Declaration of competing interest

The authors declare that they have no known competing financial interests or personal relationships that could have appeared to influence the work reported in this paper.

## 7. Acknowledgements

We acknowledge Dr. Seydou Ka for the initial screening of alkaloid from *Crinum* species and to Gabrielle Laplume for help during initiation and subculture of *C.* x *powellii* "Album" *in-vitro* tissue culture. We thank Professor Marek Mutwil and Lim Peng Ken at the Nanyang Technological University, Singapore for sharing their expertise on RNA-seq data analysis. The author contributions are MK, NM and IDP conceived, planned and designed the study. MK performed most of the experiments with the help of VK, BL, NSL and NM. MK and KCGDS conducted the bioinformatics analyses. SEG performed all the HPLC-MS/MS analysis and SR performed the GC-MS analyses. . NM and IDP supervised the study and IDP secured funding. MK, KCGDS, NM, and IDP wrote the manuscript with input from others. All authors read and approved the final version of the manuscript. All authors contributed to the article. The sequencing data was performed by Genome Québec. This research was financially supported by the Natural Sciences and Engineering Research Council of Canada (NSERC) award number RGPIN-2021-03218 to I.D-P. This work was also supported by the Canada Research Chair on plant specialized metabolism Award No 950-232164 to I.D-P. Thanks are extended to the Canadian taxpayers and to the Canadian government for supporting the Canada Research Chairs Program.

## 8. Appendix A. Supplementary data

Supplementary data to this article can be found online at …

## 9. References


Abd el Hafiz, M. A., Ramadan, M. A., Jung, M. L., Beck, J. P., Anton, R., 1991. Cytotoxic activity of Amaryllidaceae alkaloids from *Crinum augustum* and *Crinum bulbispermum*. Planta Med. 57, 437-439. https://doi.org/10.1055/s-2006-960144.

Aleya, F., Xianmin, C., Anthony, H., Meriel, J., 2021. Relative expression of putative genes involved in galanthamine and other Amaryllidaceae alkaloids biosynthesis in *Narcissus* field and in vitro tissues. Gene. 774, 145424. https://doi.org/10.1016/j.gene.2021.145424.

Anders, S., Huber, W., 2012. Differential expression of RNA-Seq data at the gene level–the DESeq package. Heidelberg, Germany: European Molecular Biology Laboratory (EMBL). 10, f1000research.

Brossi, A., Grethe, G., Teitel, S., Wildman, W. C., Bailey, D. T., 2002. Cherylline, a 4-phenyl-1,2,3,4-tetrahydroisoquinoline alkaloid. The Journal of Organic Chemistry. 35, 1100-1104. https://doi.org/10.1021/jo00829a052.

Bruex, A., Kainkaryam, R. M., Wieckowski, Y., Kang, Y. H., Bernhardt, C., Xia, Y., Zheng, X., Wang, J. Y., Lee, M. M., Benfey, P., Woolf, P. J., Schiefelbein, J., 2012. A gene regulatory network for root epidermis cell differentiation in *Arabidopsis*. PLoS Genet. 8, e1002446. https://doi.org/10.1371/journal.pgen.1002446.

Bryant, D. M., Johnson, K., DiTommaso, T., Tickle, T., Couger, M. B., Payzin-Dogru, D., Lee, T. J., Leigh, N. D., Kuo, T. H., Davis, F. G., Bateman, J., Bryant, S., Guzikowski, A. R., Tsai, S. L., Coyne, S., Ye, W. W., Freeman, R. M., Jr., Peshkin, L., Tabin, C. J., Regev, A., Haas, B. J., Whited, J. L., 2017. A Tissue-Mapped Axolotl De Novo Transcriptome Enables Identification of Limb Regeneration Factors. Cell Rep. 18, 762-776. https://doi.org/10.1016/j.celrep.2016.12.063.

Conesa, A., Madrigal, P., Tarazona, S., Gomez-Cabrero, D., Cervera, A., McPherson, A., Szczesniak, M. W., Gaffney, D. J., Elo, L. L., Zhang, X., Mortazavi, A., 2016. A survey of best practices for RNA-seq data analysis. Genome Biol. 17, 13. https://doi.org/10.1186/s13059-016-0881-8.

Demir, S. C., Yildirim, A. B., Turker, A. U., Eker, I., 2022. Seasonal variation in alkaloid content, phenolic constituent and biological activities of some *Leucojum aestivum* L. populations in Turkey. South African Journal of Botany. 147, 713-723. https://doi.org/10.1016/j.sajb.2022.03.004.

Dereeper, A., Guignon, V., Blanc, G., Audic, S., Buffet, S., Chevenet, F., Dufayard, J. F., Guindon, S., Lefort, V., Lescot, M., Claverie, J. M., Gascuel, O., 2008. Phylogeny.fr: robust phylogenetic analysis for the non-specialist. Nucleic Acids Res. 36, W465-469. https://doi.org/10.1093/nar/gkn180.

Desgagné-Penix, I., 2020. Biosynthesis of alkaloids in Amaryllidaceae plants: a review. Phytochemistry Reviews. 20, 409-431. https://doi.org/10.1007/s11101-020-09678-5.

Dewick, P. M., 2009. Medicinal natural products: a biosynthetic approach. John Wiley and Sons Ltd.

Dixon, R. A., Paiva, N. L., 1995. Stress-Induced Phenylpropanoid Metabolism. Plant Cell. 7, 1085-1097. https://doi.org/10.1105/tpc.7.7.1085.

El Tahchy, A., Bordage, S., Ptak, A., Dupire, F., Barre, E., Guillou, C., Henry, M., Chapleur, Y., Laurain-Mattar, D., 2011. Effects of sucrose and plant growth regulators on acetylcholinesterase inhibitory activity of alkaloids accumulated in shoot cultures of Amaryllidaceae. Plant Cell, Tissue and Organ Culture (PCTOC). 106, 381-390. https://doi.org/10.1007/s11240-011-9933-7.

Elgorashi, E. E., Drewes, S. E., Van Staden, J., 2002. Organ-to-organ and seasonal variation in alkaloids from *Crinum macowanii*. Fitoterapia. 73, 490-495. https://doi.org/10.1016/s0367-326x(02)00164-8.

Fennell, C. W., Elgorashi, E. E., van Staden, J., 2003. Alkaloid production in *Crinum moorei* cultures. J Nat Prod. 66, 1524-1526. https://doi.org/10.1021/np030206o.

Fennell, C. W., van Staden, J., 2001. *Crinum* species in traditional and modern medicine. J Ethnopharmacol. 78, 15-26. https://doi.org/10.1016/s0378-8741(01)00305-1.

Ferdausi, A., Chang, X., Hall, A., Jones, M., 2020. Galanthamine production in tissue culture and metabolomic study on Amaryllidaceae alkaloids in *Narcissus pseudonarcissus* cv. Carlton. Industrial Crops and Products. 144, 112058. https://doi.org/10.1016/j.indcrop.2019.112058.

Gaba, V. P., 2005. Plant growth regulators in plant tissue culture and development. Plant development and biotechnology. CRC Press Boca Raton, FL, pp. 87-99.
Gallego, A. M., Rojas, L. F., Parra, O., Rodriguez, H. A., Mazo Rivas, J. C., Urrea, A. I., Atehortua, L., Fister, A. S., Guiltinan, M. J., Maximova, S. N., Pabon-Mora, N., 2018. Transcriptomic analyses of cacao cell suspensions in light and dark provide target genes for controlled flavonoid production. Sci Rep. 8, 13575. https://doi.org/10.1038/s41598-018-31965-7.
Galperin, M. Y., Wolf, Y. I., Makarova, K. S., Vera Alvarez, R., Landsman, D., Koonin, E. V., 2021. COG database update: focus on microbial diversity, model organisms, and widespread pathogens. Nucleic Acids Res. 49, D274-D281. https://doi.org/10.1093/nar/gkaa1018.
Girard, M. P., Karimzadegan, V., Heneault, M., Cloutier, F., Berube, G., Berthoux, L., Merindol, N., Desgagne-Penix, I., 2022. Chemical Synthesis and Biological Activities of Amaryllidaceae Alkaloid Norbelladine Derivatives and Precursors. Molecules. 27, 5621. https://doi.org/10.3390/molecules27175621.
Gupta, K., Sengupta, A., Chakraborty, M., Gupta, B., 2016. Hydrogen Peroxide and Polyamines Act as Double Edged Swords in Plant Abiotic Stress Responses. Front Plant Sci. 7, 1343. https://doi.org/10.3389/fpls.2016.01343.
Haug, K., Cochrane, K., Nainala, V. C., Williams, M., Chang, J., Jayaseelan, K. V., O'Donovan, C., 2020. MetaboLights: a resource evolving in response to the needs of its scientific community. Nucleic Acids Res. 48, D440-D444. https://doi.org/10.1093/nar/gkz1019.
Hotchandani, T., de Villers, J., Desgagne-Penix, I., 2019. Developmental Regulation of the Expression of Amaryllidaceae Alkaloid Biosynthetic Genes in *Narcissus papyraceus*. Genes (Basel). 10, 594. https://doi.org/10.3390/genes10080594.
Hu, J., Li, W., Liu, Z., Zhang, G., Luo, Y., 2021. Molecular cloning and functional characterization of tyrosine decarboxylases from galanthamine-producing *Lycoris radiata*. Acta Physiologiae Plantarum. 43, 84. https://doi.org/10.1007/s11738-021-03258-6.
Hwang, I. S., Hwang, B. K., 2011. The pepper mannose-binding lectin gene CaMBL1 is required to regulate cell death and defense responses to microbial pathogens. Plant physiology. 155, 447-463.
Ieven, M., Vlietinck, A. J., Vanden Berghe, D. A., Totte, J., Dommisse, R., Esmans, E., Alderweireldt, F., 1982. Plant antiviral agents. III. Isolation of alkaloids from Clivia miniata Regel (Amaryllidaceae). J Nat Prod. 45, 564-573. https://doi.org/10.1021/np50023a009.
Ikeuchi, M., Iwase, A., Sugimoto, K., 2015. Control of plant cell differentiation by histone modification and DNA methylation. Curr Opin Plant Biol. 28, 60-67. https://doi.org/10.1016/j.pbi.2015.09.004.
Jacobowitz, J. R., Weng, J. K., 2020. Exploring Uncharted Territories of Plant Specialized Metabolism in the Postgenomic Era. Annu Rev Plant Biol. 71, 631-658. https://doi.org/10.1146/annurev-arplant-081519-035634.
Jin, Z., Yao, G., 2019. Amaryllidaceae and Sceletium alkaloids. Nat Prod Rep. 36, 1462-1488. https://doi.org/10.1039/c8np00055g.
Ka, S., Masi, M., Merindol, N., Di Lecce, R., Plourde, M. B., Seck, M., Gorecki, M., Pescitelli, G., Desgagne-Penix, I., Evidente, A., 2020. Gigantelline, gigantellinine and gigancrinine, cherylline- and crinine-type alkaloids isolated from *Crinum jagus* with anti-acetylcholinesterase activity. Phytochemistry. 175, 112390. https://doi.org/10.1016/j.phytochem.2020.112390.
Ka, S., Merindol, N., Seck, I., Ricard, S., Diop, A., Boye, C. S. B., Landelouci, K., Daoust, B., Berthoux, L., Pepin, G., Seck, M., Desgagne-Penix, I., 2021a. Biological Investigation of Amaryllidaceae Alkaloid Extracts from the Bulbs of *Pancratium trianthum* Collected in the Senegalese Flora. Molecules. 26, 7382. https://doi.org/10.3390/molecules26237382.
Ka, S., Merindol, N., Sow, A. A., Singh, A., Landelouci, K., Plourde, M. B., Pepin, G., Masi, M., Di Lecce, R., Evidente, A., Seck, M., Berthoux, L., Chatel-Chaix, L., Desgagne-Penix, I., 2021b. Amaryllidaceae Alkaloid

Cherylline Inhibits the Replication of Dengue and Zika Viruses. Antimicrob Agents Chemother. 65, e0039821. https://doi.org/10.1128/AAC.00398-21.

Khadr, A., Wang, G. L., Wang, Y. H., Zhang, R. R., Wang, X. R., Xu, Z. S., Tian, Y. S., Xiong, A. S., 2020. Effects of auxin (indole-3-butyric acid) on growth characteristics, lignification, and expression profiles of genes involved in lignin biosynthesis in carrot taproot. PeerJ. 8, e10492. https://doi.org/10.7717/peerj.10492.

Kilgore, M. B., Augustin, M. M., Starks, C. M., O'Neil-Johnson, M., May, G. D., Crow, J. A., Kutchan, T. M., 2014. Cloning and characterization of a norbelladine 4'-O-methyltransferase involved in the biosynthesis of the Alzheimer's drug galanthamine in Narcissus sp. aff. pseudonarcissus. PLoS One. 9, e103223. https://doi.org/10.1371/journal.pone.0103223.

Kilgore, M. B., Holland, C. K., Jez, J. M., Kutchan, T. M., 2016. Identification of a Noroxomaritidine Reductase with Amaryllidaceae Alkaloid Biosynthesis Related Activities. J Biol Chem. 291, 16740-16752. https://doi.org/10.1074/jbc.M116.717827.

Koirala, M., Karimzadegan, V., Liyanage, N. S., Merindol, N., Desgagne-Penix, I., 2022. Biotechnological Approaches to Optimize the Production of Amaryllidaceae Alkaloids. Biomolecules. 12, 893. https://doi.org/10.3390/biom12070893.

Lam, P. Y., Wang, L., Lo, C., Zhu, F. Y., 2022. Alternative Splicing and Its Roles in Plant Metabolism. Int J Mol Sci. 23. https://doi.org/10.3390/ijms23137355.

Langens-Gerrits, M., Albers, M., De Klerk, G.-J., 1998. Hot-water treatment before tissue culture reduces initial contamination in *Lilium* and *Acer*. Plant Cell, Tissue and Organ Culture. 52, 75-77.

Langfelder, P., Horvath, S., 2008. WGCNA: an R package for weighted correlation network analysis. BMC Bioinformatics. 9, 559. https://doi.org/10.1186/1471-2105-9-559.

Lewis, J. R., 1996. Amaryllidaceae and Sceletium alkaloids. Natural Product Reports. 13, 171-176. https://doi.org/10.1039/np9961300171.

Li, B., Dewey, C. N., 2011. RSEM: accurate transcript quantification from RNA-Seq data with or without a reference genome. BMC Bioinformatics. 12, 323. https://doi.org/10.1186/1471-2105-12-323.

Li, Q., Xu, J., Yang, L., Sun, Y., Zhou, X., Zheng, Y., Zhang, Y., Cai, Y., 2021. LED Light Quality Affect Growth, Alkaloids Contents, and Expressions of Amaryllidaceae Alkaloids Biosynthetic Pathway Genes in *Lycoris longituba*. Journal of Plant Growth Regulation. 41, 257-270. https://doi.org/10.1007/s00344-021-10298-2.

Li, W., Qiao, C., Pang, J., Zhang, G., Luo, Y., 2019. The versatile O-methyltransferase LrOMT catalyzes multiple O-methylation reactions in amaryllidaceae alkaloids biosynthesis. International journal of biological macromolecules. 141, 680-692.

Lubbe, A., Gude, H., Verpoorte, R., Choi, Y. H., 2013. Seasonal accumulation of major alkaloids in organs of pharmaceutical crop *Narcissus* Carlton. Phytochemistry. 88, 43-53. https://doi.org/10.1016/j.phytochem.2012.12.008.

Ma, L., Haile, Z. M., Sabbadini, S., Mezzetti, B., Negrini, F., Baraldi, E., 2023. Functional characterization of MANNOSE-BINDING LECTIN 1, a G-type lectin gene family member, in response to fungal pathogens of strawberry. J Exp Bot. 74, 149-161. https://doi.org/10.1093/jxb/erac396.

Majhi, B. B., Gélinas, S.-E., Mérindol, N., Desgagné-Penix, I., 2022. Characterization of norbelladine synthase and noroxomaritidine/norcraugsodine reductase reveals a novel catalytic route for the biosynthesis of Amaryllidaceae alkaloids including the Alzheimer's drug galanthamine. bioRxiv. Accepted in Frontiers in Plant Sciences Manuscript ID: 1231809, 2022.2007.2030.502154. https://doi.org/10.1101/2022.07.30.502154.

Martin, S. F., 1988. The Amaryllidaceae alkaloids., The alkaloids, vol. 30. Academic Press, p. 251.

Meerow, A. W., Lehmiller, D. J., Clayton, J. R., 2003. Phylogeny and biogeography of *Crinum* L. (Amaryllidaceae) inferred from nuclear and limited plastid non-coding DNA sequences. Botanical Journal of the Linnean Society. 141, 349-363. https://doi.org/10.1046/j.1095-8339.2003.00142.x.

Meisel, L., Fonseca, B., Gonzalez, S., Baeza-Yates, R., Cambiazo, V., Campos, R., Gonzalez, M., Orellana, A., Retamales, J., Silva, H., 2005. A rapid and efficient method for purifying high quality total RNA from peaches (*Prunus persica*) for functional genomics analyses. Biol Res. 38, 83-88. https://doi.org/10.4067/s0716-97602005000100010.

Moranska, E., Simlat, M., Warchol, M., Skrzypek, E., Waligorski, P., Laurain-Mattar, D., Spina, R., Ptak, A., 2023. Phenolic Acids and Amaryllidaceae Alkaloids Profiles in *Leucojum aestivum* L. In Vitro Plants Grown under Different Light Conditions. Molecules. 28, 1525. https://doi.org/10.3390/molecules28041525.

Nair, J. J., van Staden, J., 2023. Antiviral Effects of the Plant Family Amaryllidaceae. Natural Product Communications. 18, 1934578X231162781. https://doi.org/10.1177/1934578x231162781.

Ndakidemi, C. F., Mneney, E., Ndakidemi, P. A., 2014. Effects of Ascorbic Acid in Controlling Lethal Browning in in Vitro Culture of *Brahylaena huillensis*; Using Nodal Segments. American Journal of Plant Sciences. 05, 187-191. https://doi.org/10.4236/ajps.2014.51024.

Nino, J., Hincapie, G. M., Correa, Y. M., Mosquera, O. M., 2007. Alkaloids of *Crinum x powellii* "Album" (Amaryllidaceae) and their topoisomerase inhibitory activity. Z Naturforsch C J Biosci. 62, 223-226. https://doi.org/10.1515/znc-2007-3-411.

Park, W. T., Yeo, S. K., Sathasivam, R., Park, J. S., Kim, J. K., Park, S. U., 2020. Influence of light-emitting diodes on phenylpropanoid biosynthetic gene expression and phenylpropanoid accumulation in Agastache rugosa. Applied Biological Chemistry. 63, 25. https://doi.org/10.1186/s13765-020-00510-4.

Priyadharshini, S., Kannan, N., Manokari, M., Shekhawat, M. S., 2020. In vitro regeneration using twin scales for restoration of critically endangered aquatic plant *Crinum malabaricum* Lekhak & Yadav: a promising source of galanthamine. Plant Cell, Tissue and Organ Culture (PCTOC). 141, 593-604. https://doi.org/10.1007/s11240-020-01818-1.

Ptak, A., Tahchy, A., Skrzypek, E., Wójtowicz, T., Laurain-Mattar, D., 2013. Influence of auxins on somatic embryogenesis and alkaloid accumulation in *Leucojum aestivum* callus. Open Life Sciences. 8, 591-599. https://doi.org/10.2478/s11535-013-0160-y.

Rahimi Khonakdari, M., Rezadoost, H., Heydari, R., Mirjalili, M. H., 2020. Effect of photoperiod and plant growth regulators on in vitro mass bulblet proliferation of *Narcissus tazzeta* L. (Amaryllidaceae), a potential source of galantamine. Plant Cell Tissue Organ Culture. 142, 187-199. https://doi.org/10.1007/s11240-020-01853-y.

Rates, S. M. K., 2001. Plants as source of drugs. Toxicon. 39, 603-613. https://doi.org/10.1016/s0041-0101(00)00154-9.

Refaat, J., Kamel, M. S., Ramadan, M. A., Ali, A. A., 2012. *Crinum*; an endless source of bioactive principles: a review. Part III; *Crinum* alkaloids: Belladine-, galanthamine-, lycorenine-, tazettine-type alkaloids and other minor types. International Journal of Pharmaceutical Sciences and Research. 3, 3630. https://doi.org/10.13040/IJPSR.0975-8232.3(10).3630-38.

Saitou, N., Nei, M., 1987. The neighbor-joining method: a new method for reconstructing phylogenetic trees. Mol Biol Evol. 4, 406-425. https://doi.org/10.1093/oxfordjournals.molbev.a040454.

Singh, A., Desgagne-Penix, I., 2015. Chapter 3 : Biosynthesis of Amaryllidaceae alkaloids: A biochemical outlook. In: Alkaloids: Biosynthesis, Biological Roles and Health benefits. Nova Science Publishers.

Singh, A., Desgagne-Penix, I., 2017. Transcriptome and metabolome profiling of *Narcissus pseudonarcissus* 'King Alfred' reveal components of Amaryllidaceae alkaloid metabolism. Sci Rep. 7, 17356. https://doi.org/10.1038/s41598-017-17724-0.

Singh, A., Massicotte, M. A., Garand, A., Tousignant, L., Ouellette, V., Berube, G., Desgagne-Penix, I., 2018. Cloning and characterization of norbelladine synthase catalyzing the first committed reaction in Amaryllidaceae alkaloid biosynthesis. BMC Plant Biol. 18, 338. https://doi.org/10.1186/s12870-018-1570-4.

Slabbert, M., De Bruyn, M., Ferreira, D., Pretorius, J., 1993. Regeneration of bulblets from twin scales of *Crinum macowanii* in vitro. Plant cell, tissue and organ culture. 33, 133-141. https://doi.org/10.1007/BF01983226.

Tallini, L. R., Osorio, E. H., Santos, V. D. D., Borges, W. S., Kaiser, M., Viladomat, F., Zuanazzi, J. A. S., Bastida, J., 2017. *Hippeastrum reticulatum* (Amaryllidaceae): Alkaloid Profiling, Biological Activities and Molecular Docking. Molecules. 22, 4901. https://doi.org/10.3390/molecules22122191.

Tallini, L. R., Torras-Claveria, L., Borges, W. S., Kaiser, M., Viladomat, F., Zuanazzi, J. A. S., Bastida, J., 2018. N-oxide alkaloids from *Crinum amabile* (Amaryllidaceae). Molecules. 23, 1277. https://doi.org/10.3390/molecules23061277.

Tamura, K., Stecher, G., Kumar, S., 2021. MEGA11: Molecular Evolutionary Genetics Analysis Version 11. Mol Biol Evol. 38, 3022-3027. https://doi.org/10.1093/molbev/msab120.

Tang, M., Li, C., Zhang, C., Cai, Y., Zhang, Y., Yang, L., Chen, M., Zhu, F., Li, Q., Li, K., 2023. SWATH-MS-Based Proteomics Reveals the Regulatory Metabolism of Amaryllidaceae Alkaloids in Three *Lycoris* Species. Int J Mol Sci. 24. https://doi.org/10.3390/ijms24054495.

Taylor-Teeples, M., Lin, L., de Lucas, M., Turco, G., Toal, T. W., Gaudinier, A., Young, N. F., Trabucco, G. M., Veling, M. T., Lamothe, R., Handakumbura, P. P., Xiong, G., Wang, C., Corwin, J., Tsoukalas, A., Zhang, L., Ware, D., Pauly, M., Kliebenstein, D. J., Dehesh, K., Tagkopoulos, I., Breton, G., Pruneda-Paz, J. L., Ahnert, S. E., Kay, S. A., Hazen, S. P., Brady, S. M., 2015. An *Arabidopsis* gene regulatory network for secondary cell wall synthesis. Nature. 517, 571-575. https://doi.org/10.1038/nature14099.

Tousignant, L., Diaz-Garza, A. M., Majhi, B. B., Gelinas, S. E., Singh, A., Desgagne-Penix, I., 2022. Transcriptome analysis of *Leucojum aestivum* and identification of genes involved in norbelladine biosynthesis. Planta. 255, 30. https://doi.org/10.1007/s00425-021-03741-x.

Trujillo Chacón, L. M., Leiva, H., Zapata Vahos, I. C., Restrepo, D. C., Osorio, E., 2023. Influence of plant growth regulators on in vitro biomass production and biosynthesis of cytotoxic Amaryllidaceae alkaloids in *Caliphuria tenera* Baker. Biocatalysis and Agricultural Biotechnology. 50, 102670. https://doi.org/10.1016/j.bcab.2023.102670.

Trujillo-Chacon, L. M., Pastene-Navarrete, E. R., Bustamante, L., Baeza, M., Alarcon-Enos, J. E., Cespedes-Acuna, C. L., 2020. In vitro micropropagation and alkaloids analysis by GC-MS of Chilean Amaryllidaceae plants: *Rhodophiala pratensis*. Phytochem Anal. 31, 46-56. https://doi.org/10.1002/pca.2865.

Velten, R., Erdelen, C., Gehling, M., Göhrt, A., Gondol, D., Lenz, J., Lockhoff, O., Wachendorff, U., Wendisch, D., 1998. Cripowellin A and B, a novel type of Amaryllidaceae alkaloid from *Crinum powellii*. Tetrahedron Letters. 39, 1737-1740. https://doi.org/10.1016/S0040-4039(98)00057-4.

Wang, R., Xu, S., Wang, N., Xia, B., Jiang, Y., Wang, R., 2016. Transcriptome Analysis of Secondary Metabolism Pathway, Transcription Factors, and Transporters in Response to Methyl Jasmonate in *Lycoris aurea*. Front Plant Sci. 7, 1971. https://doi.org/10.3389/fpls.2016.01971.

Wang, W., Chen, Z.-D., 2007. Generic level phylogeny of Thalictroideae (Ranunculaceae) - implications for the taxonomic status of *Paropyrum* and petal evolution. Taxon. 56, 811-821. https://doi.org/10.2307/25065863.

Wink, M., 2008. Ecological roles of alkaloids. Wiley Online Library, pp. 3-52.

Winkel-Shirley, B., 2001. Flavonoid biosynthesis. A colorful model for genetics, biochemistry, cell biology, and biotechnology. Plant Physiol. 126, 485-493. https://doi.org/10.1104/pp.126.2.485.

Woodward, A. W., Bartel, B., 2005. Auxin: regulation, action, and interaction. Ann Bot. 95, 707-735. https://doi.org/10.1093/aob/mci083.

Xu, J., Li, Q., Yang, L., Li, X., Wang, Z., Zhang, Y., 2020. Changes in carbohydrate metabolism and endogenous hormone regulation during bulblet initiation and development in *Lycoris radiata*. BMC Plant Biol. 20, 180. https://doi.org/10.1186/s12870-020-02394-4.

Yoda, H., Yamaguchi, Y., Sano, H., 2003. Induction of hypersensitive cell death by hydrogen peroxide produced through polyamine degradation in tobacco plants. Plant Physiology. 132, 1973-1981. https://doi.org/10.1104/pp.103.024737.

Zhan, J., Thakare, D., Ma, C., Lloyd, A., Nixon, N. M., Arakaki, A. M., Burnett, W. J., Logan, K. O., Wang, D., Wang, X., Drews, G. N., Yadegari, R., 2015. RNA sequencing of laser-capture microdissected compartments of the maize kernel identifies regulatory modules associated with endosperm cell differentiation. Plant Cell. 27, 513-531. https://doi.org/10.1105/tpc.114.135657.

# Auxin and light-mediated regulation of growth, morphogenesis, and alkaloid biosynthesis in *Crinum* x *powellii* 'Album' callus

Manoj Koirala [1], Karen Cristine Goncalves dos Santos [1], Sarah-Eve Gélinas [1], Simon Ricard [1], Vahid Karimzadegan [1], Basanta Lamichhane [1], Nuwan Sameera Liyanage [1], Natacha Merindol [1], Isabel Desgagné-Penix [1,2]

[1] Department of Chemistry, Biochemistry and Physics, Université du Québec à Trois-Rivières, Trois-Rivières, QC, Canada

[2] Plant Biology Research Group, Trois-Rivières, Québec, Canada

* Corresponding author's email address: Isabel.Desgagne-Penix@uqtr.ca (Isabel Desgagné-Penix)

## Highlights

- *Crinum* x *powellii* 'Album' produces a wide range of Amaryllidaceae alkaloids (AAs).
- Auxin and light both regulate tissue differentiation and AAs biosynthesis.
- Multi-omics analysis enabled the identification of candidate genes of AA biosynthesis.
- Equilibrium of growth and stress is important for sustainable production of AA.

# Auxin and light-mediated regulation of growth, morphogenesis, and alkaloid biosynthesis in *Crinum* x *powellii* 'Album' callus

Manoj Koirala [1], Karen Cristine Goncalves dos Santos [1], Sarah-Eve Gélinas [1], Simon Ricard [1], Vahid Karimzadegan [1], Basanta Lamichhane [1], Nuwan Sameera Liyanage [1], Natacha Merindol [1], Isabel Desgagné-Penix [1,2]

[1] Department of Chemistry, Biochemistry and Physics, Université du Québec à Trois-Rivières, Trois-Rivières, QC, Canada

[2] Plant Biology Research Group, Trois-Rivières, Québec, Canada



## Declaration of interest statement

The authors declare that they have no known competing financial interests or personal relationships that could have appeared to influence the work reported in this paper.